iScience

CellPress
OPEN ACCESS

Article

# Global isonicotinylome analysis identified SMAD3 isonicotinylation promotes liver cancer cell epithelial–mesenchymal transition and invasion

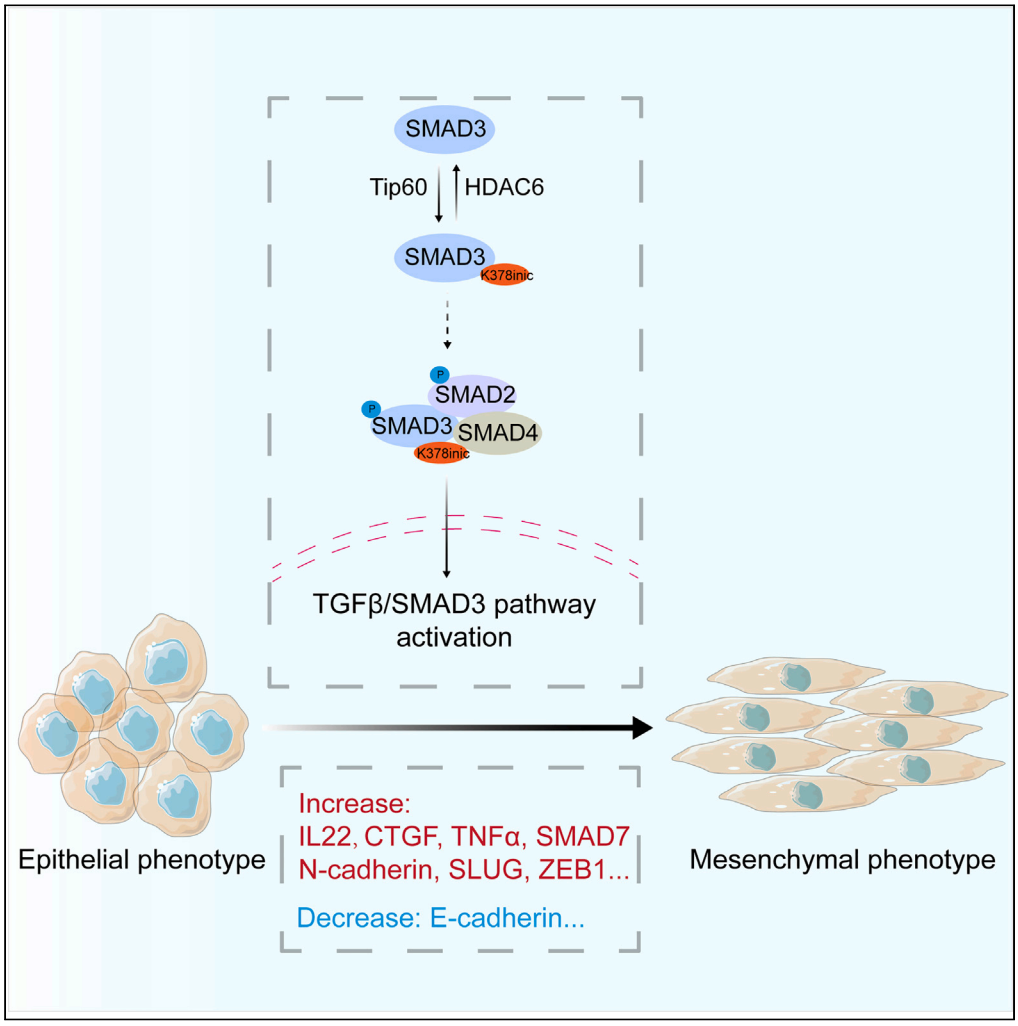


Yixiao Li, Yuhan Jiang, Haoyi Yan, Ziheng Qin, Yidi Peng, Danyu Lv, Hongquan Zhang

hongquan.zhang@bjmu.edu.cn

## Highlights

11442 Kinic sites of 2792 proteins identified in global isonicotinylome analysis

Tip60 and HDAC6 are the isonicotinyl-transferase and deisonicotinylase of SMAD3

K378inic activates SMAD3 and promotes HCC cells EMT and invasion

Li et al., iScience 27, 110775
September 20, 2024 
https://doi.org/10.1016/j.isci.2024.110775

iScience

CellPress
OPEN ACCESS

Article

# Global isonicotinylome analysis identified SMAD3 isonicotinylation promotes liver cancer cell epithelial–mesenchymal transition and invasion

Yixiao Li,[1,2] Yuhan Jiang,[1,2] Haoyi Yan,[1] Ziheng Qin,[1] Yidi Peng,[1] Danyu Lv,[1] and Hongquan Zhang[1,3,*]

## SUMMARY

**Histone lysine isonicotinylation (Kinic) induced by isoniazid (INH) was recently identified as a post-translational modification in cells. However, global cellular non-histone proteins Kinic remains unclear. Using proteomic technology, we identified 11,442 Kinic sites across 2,792 proteins and demonstrated that Kinic of non-histone proteins is involved in multiple function pathways. Non-histone proteins Kinic can be regulated by isonicotinyl-transferases, including CBP and Tip60, and deisonicotinylases, including HDAC8 and HDAC6. In particular, the Kinic of poly (ADP-ribose) (PAR) polymerase 1 (PARP1) can be catalyzed by CBP and deisonicotinylation can be catalyzed by HDAC8. Tip60 and HDAC6 are isonicotinyl-transferase and the deisonicotinylase of SMAD3, respectively. Importantly, we found the K378inic of SMAD3 increases its phosphorylation, activates TGFβ pathway, and promotes liver cancer cells migration and invasion. In conclusion, our study demonstrated non-histone proteins Kinic occur extensively in cells and plays an important role in regulation of various cellular functions, including cancer progression.**

## INTRODUCTION

Recently, with the development of high-sensitivity mass spectrometry (MS), a series of protein post-translational modifications (PTMs) have been identified such as histone lysine crotonylation, succinylation, and lactylation.[1–4] Histone PTMs are crucial epigenetic mechanisms that regulate chromatin dynamics and gene expression.[5,6] Non-histone protein PTMs are also important and are involved in key cellular processes relevant to physiology and disease, such as gene transcription, DNA damage repair, cell division, signal transduction, protein folding, autophagy, and metabolism.[7]

Histone Kinic was previously identified as a novel acylation modification that occurs on histones. It can be induced by the anti-tuberculosis drug INH or its downstream metabolite isonicotinic acid and promotes genes associated with tumor expression by increasing chromatin accessibility in hepatocellular carcinoma. Additionally, CBP/p300 and HDAC3 are the writers and eraser of histone Kinic, respectively.[8] However, writers and erasers of non-histone protein Kinic remain unknown.

The transforming growth factor β (TGFβ) pathway, as an important signal pathway in proliferation, migration, collagen synthesize, and epithelial-mesenchymal transition (EMT), is responsible for many key proteins and kinases.[9] SMAD3 is a crucial member of the SMADs family and plays a central role in the TGFβ pathway.[10] When the TGFβ pathway is activated, SMAD3 is phosphorylated by the TGFβ receptor I, forming a complex with SMAD2/SMAD4 in the cytoplasm.[11,12] This complex is then transported into nucleus, where the SMADs complex binds to promoter of target genes such as *IL-22*, *CTGF*, *TNFα*, and *SMAD7*.[13–15] To date, multiple PTMs of SMAD3 been reported, including methylation, ubiquitination, and acetylation, which have different effects on SMAD3 activation, translocation, and stability.[14,16–18] However, the presence and impact of Kinic on SMAD3 within the TGFβ pathway remain to be explored.

In this study, we used MS analysis to identify histones and many non-histone Kinic substrates, including PARP1 and SMAD3. We also demonstrated that Kinic is a widespread modification involved in various cellular metabolic processes. In particular, the K378inic of SMAD3 is crucial for phosphorylation, and nuclear translocation. Furthermore, our data showed that Kinic of SMAD3 promotes the migration and invasion of liver cancer cells by activating the TGFβ pathway and EMT.

## RESULTS

### Identification of global Kinic status in HeLa cells

We previously reported that the anti-tuberculosis drug INH induces Kinic.[8] HeLa cells were treated with 10 mM INH, and the results showed that the whole protein Kinic level was significantly increased (Figure 1A). To gain a global view of the INH-induced isonicotinylome, especially

[1]Program for Cancer and Cell Biology, Department of Human Anatomy, Histology and Embryology, School of Basic Medical Sciences, Peking University International Cancer Institute, State Key Laboratory of Molecular Oncology, Peking University Health Science Center, Beijing 100191, China
[2]These authors contributed equally
[3]Lead contact
*Correspondence: hongquan.zhang@bjmu.edu.cn
https://doi.org/10.1016/j.isci.2024.110775

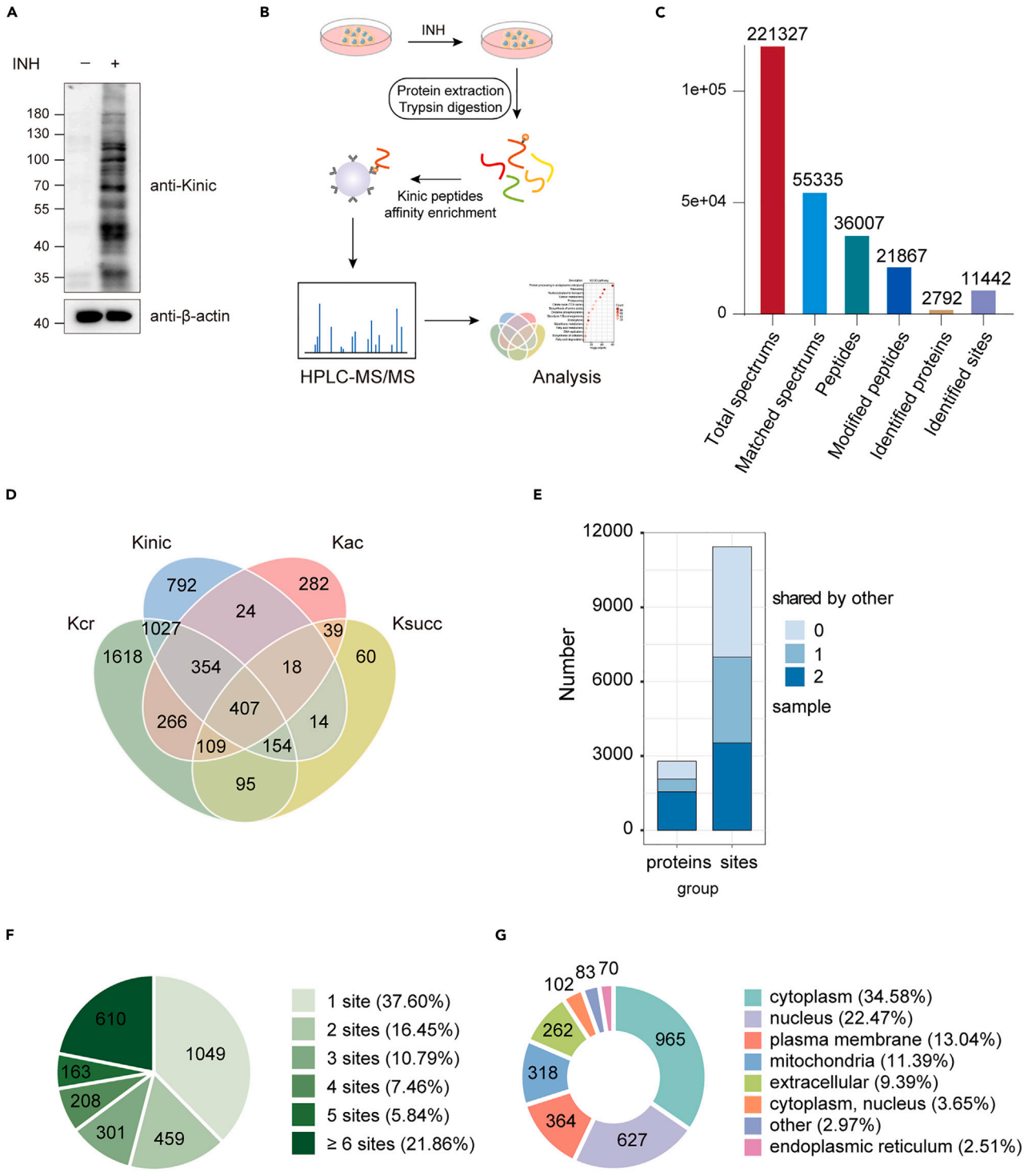


**Figure 1. Identification of global Kinic status in HeLa cells**

(A) Western blot assay with whole-cell lysates from HeLa cells treated with or without INH and tested using pan-Kinic antibody.

(B) Schematic of the experimental design of proteomics via which to map isonicotinylated peptides.

(C) Statistical analysis of isonicotinylated peptides in proteomic of HeLa cells.

(D) Venn diagram of different modifications (Kinic, Kcr, Kac, and Ksucc) sites intersection in HeLa cells.

(E) Bar chart of the number of proteins or sites in three repeat samples.

(F) Pie chart of the number distribution of sites for isonicotinylated proteins in proteomic.

(G) Donut chart of the subcellular distribution of isonicotinylated proteins in proteomic.

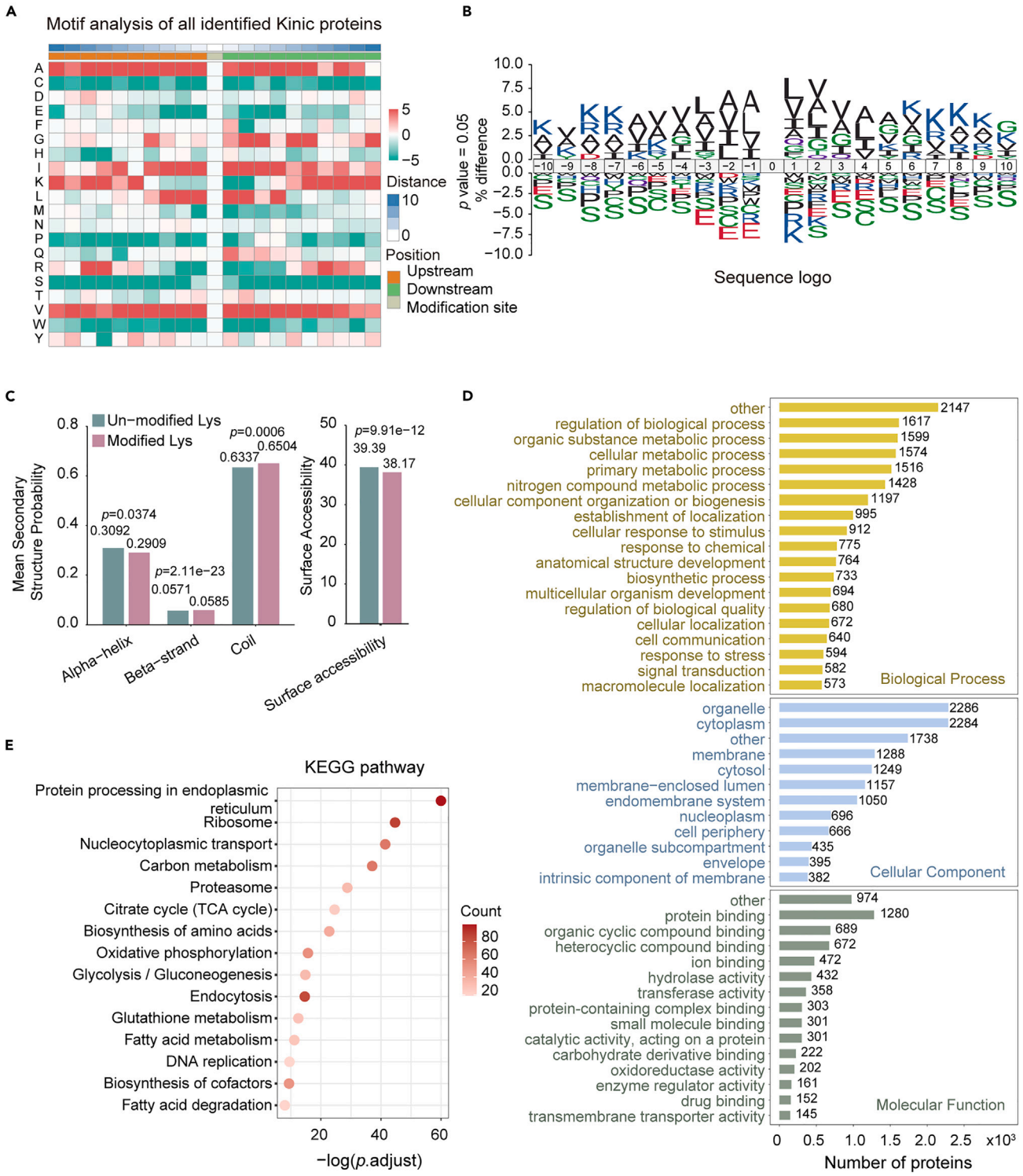


**Figure 2. The functional characterization of isonicotinylated proteins**

(A) Heatmap showing the ten amino acids at each position flanking the Kinic sites. Red represents enrichment, and green represents depletion.

(B) Motif analysis of flanking sequence preference for all Kinic sites by IceLogo representation.

(C) Distribution of all lysine and isonicotinylated lysine in structured regions of proteins.

(D) The presentation of GO annotations enriched with Kinic proteome.

(E) The presentation of KEGG pathways annotations enriched with Kinic proteome.

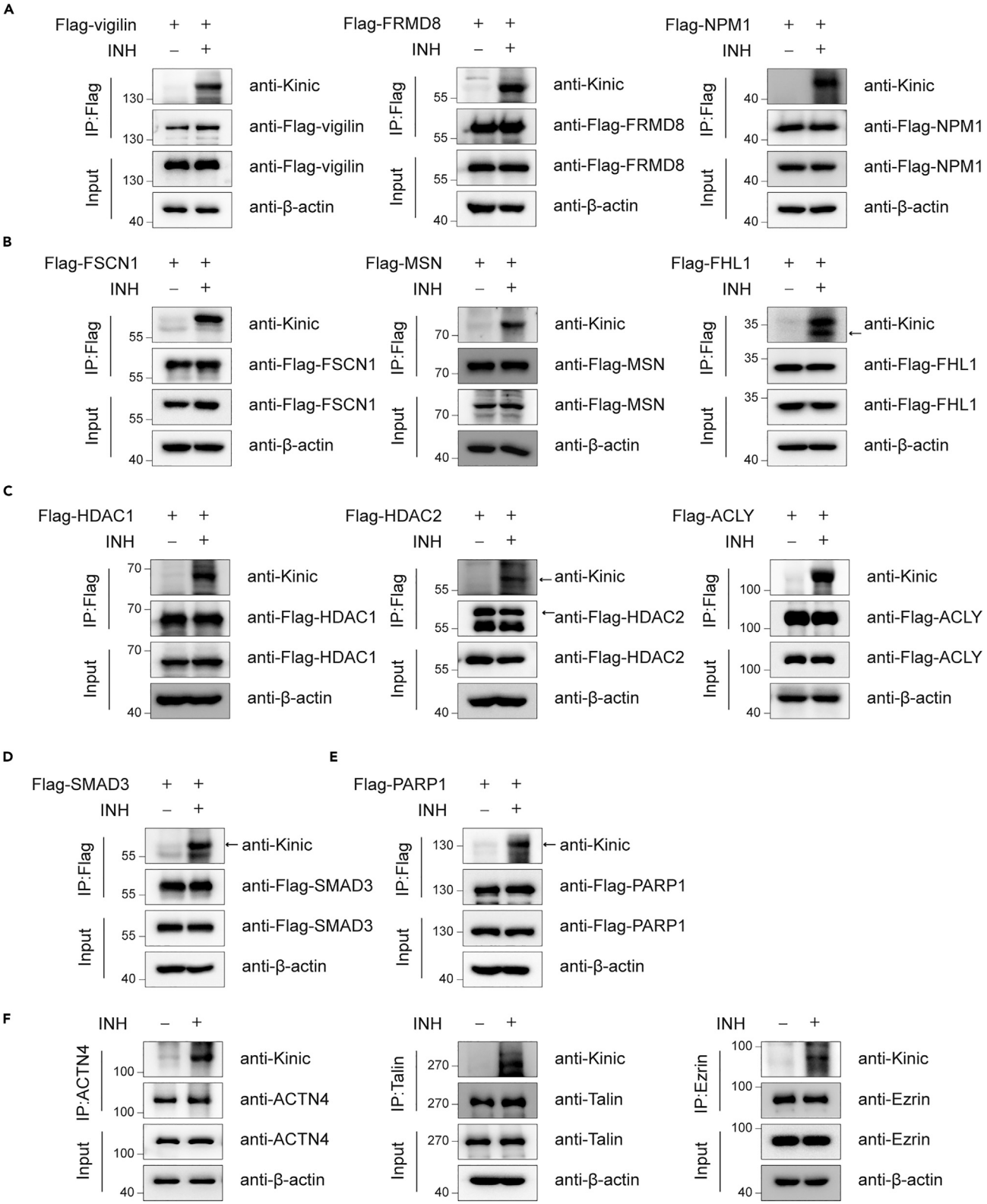
A
Flag-vigilin + +
INH – +
IP:Flag
130
anti-Kinic
130
anti-Flag-vigilin
Input
130
anti-Flag-vigilin
40
anti-β-actin
Flag-FRMD8 + +
INH – +
IP:Flag
55
anti-Kinic
55
anti-Flag-FRMD8
Input
55
anti-Flag-FRMD8
40
anti-β-actin
Flag-NPM1 + +
INH – +
IP:Flag
40
anti-Kinic
40
anti-Flag-NPM1
Input
40
anti-Flag-NPM1
40
anti-β-actin
B
Flag-FSCN1 + +
INH – +
IP:Flag
55
anti-Kinic
55
anti-Flag-FSCN1
Input
55
anti-Flag-FSCN1
40
anti-β-actin
Flag-MSN + +
INH – +
IP:Flag
70
anti-Kinic
70
anti-Flag-MSN
Input
70
anti-Flag-MSN
40
anti-β-actin
Flag-FHL1 + +
INH – +
IP:Flag
35
anti-Kinic
35
anti-Flag-FHL1
Input
35
anti-Flag-FHL1
40
anti-β-actin
C
Flag-HDAC1 + +
INH – +
IP:Flag
70
anti-Kinic
70
anti-Flag-HDAC1
Input
70
anti-Flag-HDAC1
40
anti-β-actin
Flag-HDAC2 + +
INH – +
IP:Flag
55
anti-Kinic
55
anti-Flag-HDAC2
Input
55
anti-Flag-HDAC2
40
anti-β-actin
Flag-ACLY + +
INH – +
IP:Flag
100
anti-Kinic
100
anti-Flag-ACLY
Input
100
anti-Flag-ACLY
40
anti-β-actin
D
Flag-SMAD3 + +
INH – +
IP:Flag
55
anti-Kinic
55
anti-Flag-SMAD3
Input
55
anti-Flag-SMAD3
40
anti-β-actin
E
Flag-PARP1 + +
INH – +
IP:Flag
130
anti-Kinic
130
anti-Flag-PARP1
Input
130
anti-Flag-PARP1
40
anti-β-actin
F
INH – +
IP:ACTN4
100
anti-Kinic
100
anti-ACTN4
Input
100
anti-ACTN4
40
anti-β-actin
INH – +
IP:Talin
270
anti-Kinic
270
anti-Talin
Input
270
anti-Talin
40
anti-β-actin
INH – +
IP:Ezrin
100
anti-Kinic
100
anti-Ezrin
Input
100
anti-Ezrin
40
anti-β-actin

**Figure 3. Verification of Kinic in non-histone proteins**

(A–E) HeLa cells transfected with Flag-tagged vigilin, FRMD8, NPM1, FSCN1, MSN, FHL1, HDAC1, HDAC2, ACLY, SMAD3, and PARP1 plasmids were treated with 10 mM INH for 24 h, and then cell lysates were subjected to IP with M2 beads, determined by Western blotting with indicated antibodies.

(F) HeLa cells were treated with 10 mM INH for 24 h, and then cell lysates were subjected to IP with anti-ACTN4, anti-Talin, and anti-Ezrin antibodies, determined by western blotting with indicated antibodies.

the Kinic of non-histone proteins substrates, we used pan-antibody-conjugated beads to enrich modified peptides prior to high-resolution liquid chromatography-tandem MS analysis to investigate Kinic substrates upon stimulation of INH in HeLa cells (Figure 1B). A total of 11,442 sites on 2,792 proteins were identified to be isonicotinylated after INH treatment (Figure 1C) (Table S1), but a total of 44 sites on 35 proteins were identified to be isonicotinylated without INH treatment (Figure S1A) (Table S2). To investigate whether the proteomic distribution of Kinic overlaps with that of other lysine acylations, lysine Kinic sites were compared with previously determined lysine acetylation (Kac), succinylation (Ksucc), and crotonylation (Kcr) sites in HeLa cells.[19,20] The results revealed 407 overlapping sites among Kinic, Kcr, Kac, and Ksucc, along with 1,942 overlapping sites between Kinic and Kcr, 803 between Kinic and Kac, and 593 between Kinic and Ksucc, suggesting distinct biological roles for these acylations (Figure 1D). Figure 1E illustrates the quantitative distribution of proteins and sites with Kinic modifications. Among these Kinic proteins, 1,809 (64.84%) had fewer than four Kinic sites (Figure 1F). We also determined the subcellular distribution of these Kinic proteins. The results showed that a large proportion of Kinic proteins were localized in the cytoplasm (34.58%), nucleus (22.47%), plasma membrane (13.04%), and mitochondria (11.39%). These results indicated that cellular protein Kinic is widely distributed within HeLa cells.

## Functional characterization of isonicotinylated proteins

To understand the consensus motif preference of the Kinic, we analyzed the amino acids flanking the Kinic sites using IceLogo. The amino acid composition surrounding Kinic sites was notably enriched with hydrophobic residues (alanine, leucine, valine, isoleucine), and glycine, resembling the pattern observed in β-hydroxybutyrylation.[21] Conversely, polar uncharged amino acids and negatively charged glutamic acid were excluded (Figures 2A and 2B). Structural analysis via Netsurf showed that the distribution of Kinic sites were preferentially located in disordered coils. The average surface accessibility of protein Kinic was slightly lower than that of the total lysine residues, suggesting a preference for locations within protein structures (Figure 2C). To understand the biological functions of the Kinic substrates, the cellular components of isonicotinylated proteins were classified according to their molecular functions and biological processes based on Gene Ontology (GO) annotation and Kyoto Encyclopedia of Genes and Genomes (KEGG) analysis. GO analysis indicated that the Kinic proteins were enriched in the regulation of biological processes, organic substance metabolism, and cellular metabolism (Figure 2D). KEGG pathway analysis highlighted enrichment of isonicotinylated proteins in various pathways, including protein processing in the endoplasmic reticulum, ribosome, nucleocytoplasmic transport, carbon metabolism, and the TCA cycle (Figures 2E and S1B). These results indicated that Kinic may play a key role in the coordination of different metabolic pathways in response to tumor conditions.

## Verification of isonicotinylation in non-histone proteins

To validate the isonicotinylated proteins identified via MS, we selected 11 proteins and detected their Kinic levels through immunoprecipitation (IP) after treatment with 10 mM INH. These substrate proteins were associated with different metabolic processes, such as tumor invasion and metastasis (including vigilin, FRMD8, and NPM1) (Figure 3A), cell signaling transduction (including FSCN1, MSN, and FHL1) (Figure 3B), epigenetic modification-associated enzymes (including HDAC1, HDAC2, and ACLY) (Figure 3C), the TGFβ signaling pathway (including SMAD3) (Figure 3D), and repair of DNA damage-associated proteins (including PARP1) (Figure 3E). The IP results showed that these substrates underwent significant Kinic after INH treatment. Furthermore, we used antibodies against endogenous proteins (ACTN4, Talin, and Ezrin) to perform IP experiments to detect Kinic. As expected, they were isonicotinylated by INH (Figure 3F). Therefore, we conclude that Kinic can occur on certain non-histone proteins in addition to histones within cells.

## CBP isonicotinylates, whereas HDAC8 deisonicotinylates PARP1

DNA damage is a universal phenomenon in many biological processes, particularly tumorigenesis.[22] Double-strand break is one of the most common types of DNA damage detected by PARP1.[23] Following the verification of PARP1 Kinic in Figure 3E, we proceeded with an in-depth investigation of non-histone protein Kinic, using PARP1 as an example. Drawing from prior research indicating a potential shared enzymatic system between Kinic and acetylation modification,[8] we co-transfected PARP1 with a panel of acetyltransferases including CBP, p300, hMOF, KAT7, and Tip60. The results showed that PARP1 was isonicotinylated by CBP (Figures 4A and 4B). Conversely, the Kinic level of PARP1 was significantly decreased when endogenous CBP was knocked down using siRNA (Figure 4C). An interaction between PARP1 and CBP was observed in cells, with both proteins exhibiting colocalization within the nucleus (Figures 4D and 4E). Therefore, we conclude that CBP is responsible for the Kinic of PARP1.

We ectopically expressed PARP1 and treated cells with trichostatin A (TSA), an inhibitor of HDAC family deacetylases, and nicotinamide (NAM), an inhibitor of SIRT family deacetylases. The results showed that Kinic of PARP1 was significantly enhanced after treatment with TSA, but not with NAM (Figure 4F). Therefore, we narrowed down the range of deisonicotinylases of PARP1 to the HDAC family. Through overexpressing PARP1 and transfecting with various of HDACs, we found that inhibitors targeting HDAC8/10, as well as the broad-spectrum HDAC inhibitors CAY10603 or NaBu, led to enhanced the Kinic of PARP1 (Figure 4G). In addition, we carried out IP experiments with PARP1 and HDAC members including HDAC1-10 and found that PARP1 was deisonicotinylated by HDAC3, HDAC4, HDAC5, and HDAC8

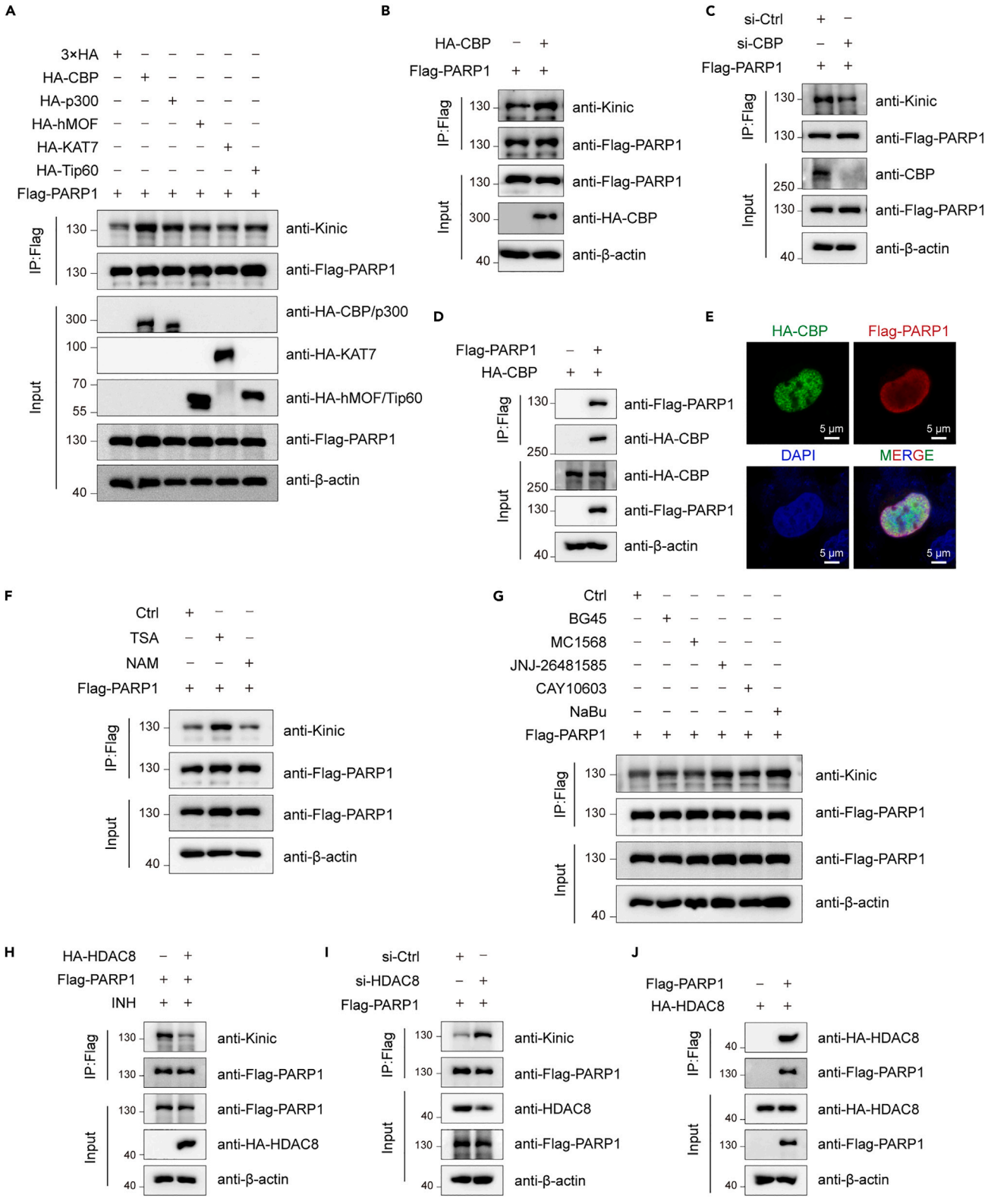


**Figure 4. CBP and HDAC8 are the Kinic regulatory enzymes of PARP1**

(A) Transfected with Flag-PARP1 and 3×HA or HA-tagged CBP, p300, hMOF, KAT7, and Tip60 for 48h, HEK293T cell lysates were subjected to IP with M2 beads, and then determined by Western blotting with indicated antibodies.

**Figure 4. *Continued***

(B) Transfected Flag-PARP1 and HA-tagged CBP for 48h, HEK293T cell lysates were subjected to IP with M2 beads, and then determined by Western blotting with indicated antibodies.

(C) Transfected Flag-PARP1 after knockdown of CBP by siRNA, HEK293T cell lysates were subjected to IP with M2 beads, and then determined by Western blotting with indicated antibodies.

(D) Transfected with Flag-PARP1 and HA-tagged CBP, HEK293T cell lysates were subjected to IP with M2 beads, and then determined by Western blotting with indicated antibodies.

(E) HeLa cells were transfected Flag-PARP1 and HA-tagged CBP, the position of protein expression was detected by immunofluorescence. followed by visualization with confocal microscopy, Scale bar, 5 μm.

(F) Transfected Flag-PARP1 and treated with TSA or NAM, HEK293T cell lysates were subjected to IP with M2 beads, and then determined by Western blotting with indicated antibodies.

(G) HEK293T cells were transfected Flag-PARP1 and treated with diverse inhibitor of HDACs. HDAC1/2/3 inhibitor: BG45, HDAC4/5/7/9 inhibitor: MC1568, HDAC8/10 inhibitor: JNJ-26481585, All HDACs inhibitor: CAY10603 or NaBu. Cell lysates were subjected to IP with M2 beads, and then determined by Western blotting with indicated antibodies.

(H) Transfected with Flag-PARP1 and HA-tagged HDAC8 for 48h, HEK293T cell lysates were subjected to IP with M2 beads, and then determined by Western blotting with indicated antibodies.

(I) Transfected Flag-PARP1 after knockdown of HDAC8 by siRNA, HEK293T cell lysates were subjected to IP with M2 beads, and then determined by Western blotting with indicated antibodies.

(J) Transfected with Flag-PARP1 and HA-tagged HDAC8, HEK293T cell lysates were subjected to IP with M2 beads, and then determined by Western blotting with indicated antibodies.

(Figure S2A). Consequently, our focus shifted toward HDAC8. Co-expression of PARP1 with HDAC8 resulted in a dramatic decrease in the level of PARP1 Kinic (Figure 4H). In contrast, the Kinic level of PARP1 significantly increased with endogenous knockdown of HDAC8 using siRNA (Figure 4I). In addition, PARP1 and HDAC8 interacted with each other within the cells (Figure 4J). In summary, the acetyltransferase CBP acts as an isonicotinyl-transferase for PARP1, and HDAC8 is the major deisonicotinylase for PARP1.

## Tip60 isonicotinylates, whereas HDAC6 deisonicotinylates SMAD3

Another notable example of non-histone protein Kinic involves SMAD3, a pivotal member of the SMADs signaling cascade and TGFβ pathway. SMAD3 plays a crucial role in regulating several cellular processes, including cell differentiation, growth, migration, extracellular matrix production, and EMT.[9] Figure 3D shows that SMAD3 can be isonicotinylated; however, the acyltransferase that mediates the Kinic of SMAD3 remains unclear. Primarily, we found that SMAD3 interacted with a variety of acyltransferases in cells, including hMOF, Tip60, KAT7, and PCAF (Figure S3A). We then co-transfected SMAD3 with acetyltransferases hMOF, PCAF, Tip60, and KAT7. The results showed that SMAD3 was significantly isonicotinylated by Tip60 (Figure 5A). The Kinic levels of SMAD3 exhibited a dose-dependent increase with Tip60 stimulation (Figure 5B). Conversely, the Kinic level of SMAD3 significantly decreased with the knockdown of Tip60 by siRNA (Figure 5C). Therefore, Tip60 is responsible for the Kinic of SMAD3.

We also found that the Kinic level of SMAD3 was significantly enhanced after treatment with TSA, but not with NAM (Figure 5D). In contrast to PARP1, co-expression of SMAD3 with HDACs revealed that HDAC6 can deisonicotinylate SMAD3 (Figures 5E and 5F). While knocking down the HDAC6 expression by siRNA, the Kinic level of SMAD3 significantly increased (Figure 5G). SMAD3 and HDAC6 interacted with each other in cells, as detected by co-IP (Figure 5H). In summary, the acetyltransferase Tip60 acts as an isonicotinyl-transferase for SMAD3, and HDAC6 is the major deisonicotinylase of SMAD3 in cells.

## K378 is the major isonicotinylation site of SMAD3

INH induced the Kinic of SMAD3 in a concentration-dependent manner (Figure 6A). Endogenous SMAD3 can also undergo Kinic in response to INH (Figure 6B). Non-histone proteins are susceptible to various acylation modifications, which can induce epigenetic changes by regulating protein stability, activity, localization, and dynamic interactions with other cellular molecules such as nucleic acids, lipids, and cofactors.[7] Interestingly, INH markedly increased the Kinic of SMAD3 but significantly decreased its ubiquitylation (Figure 6C). However, when treated with INH, there was no change in SMAD3 protein stability, as ubiquitination decreased (Figure 6D). Previous studies have demonstrated that SMAD3 possesses six ubiquitination sites. Ubiquitination at these sites does not affect protein stability.[24,25] The sequence of the conservation analysis results for SMAD3 indicated that the six sites were highly conserved across species from *Gallus* to *Homo sapiens* (Figures 6E, S4A, and S4B). We hypothesized that the ubiquitin site was occupied by Kinic, and thus, ubiquitination was reduced. Therefore, six SMAD3 mutants were constructed (SMAD3-K33R, K53R, K81R, K333R, K378R, and K409R) in which the lysine sites were substituted with arginine and were therefore unsuitable for Kinic. As shown in Figure 6F, with 10 mM INH treatment, SMAD3-K33R and K378R led to a marked reduction of Kinic. However, as the INH concentration increased to 20 mM, only K378R and K33/378R showed reduced Kinic levels (Figures 6G and S4C). Therefore, we concluded that the main Kinic site of SMAD3 was K378.

## K378inic is required for SMAD3 promoting liver cancer cell migration, invasion, and EMT

SMADs family members play crucial roles in the TGFβ pathway, which is pivotal for EMT and collagen synthesis.[26] After being phosphorylated, SMAD family members migrate to the nucleus, where they contribute to the activation or inhibition of different genes.[27] We selected normal

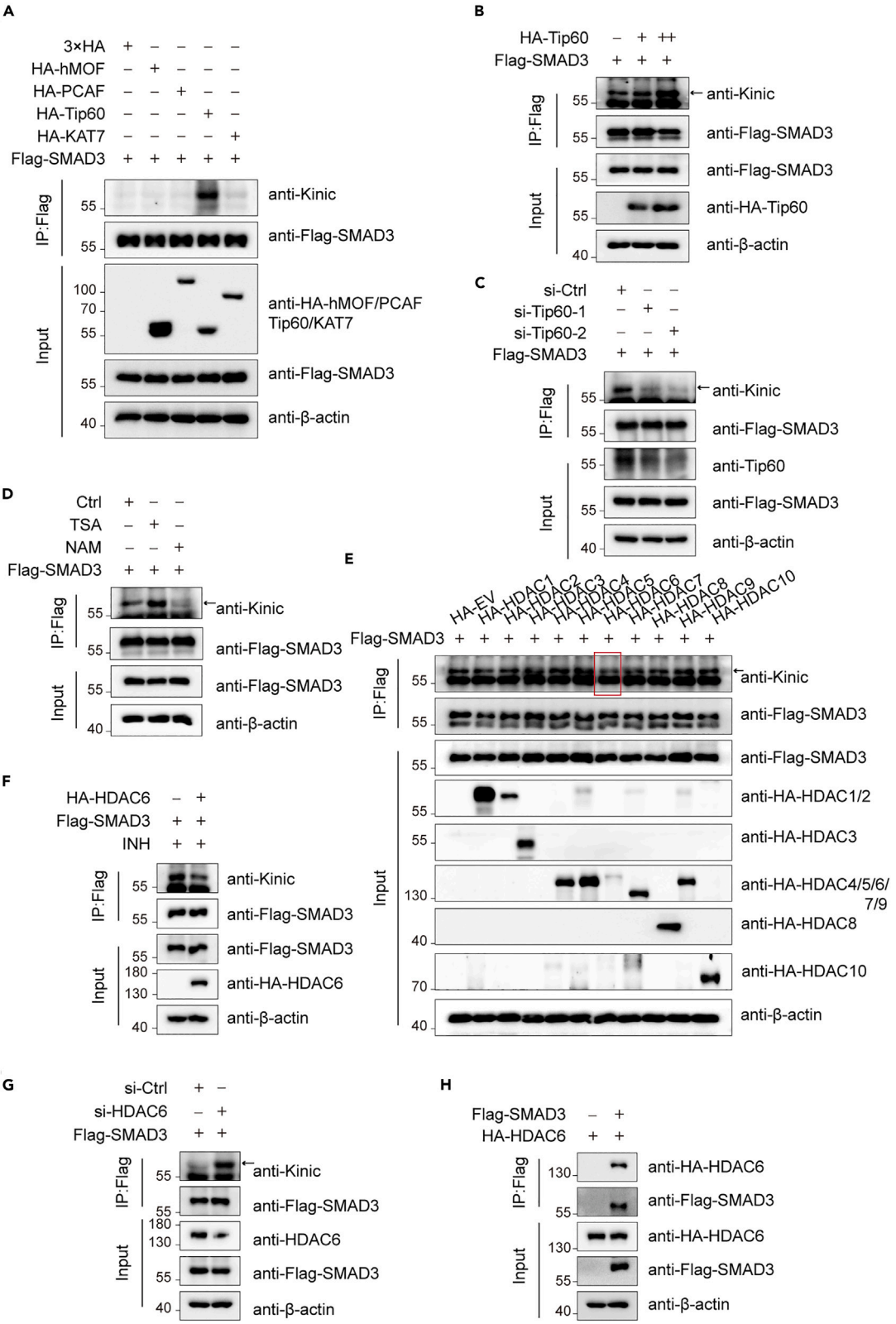
A
3×HA + – – – –
HA-hMOF – + – – –
HA-PCAF – – + – –
HA-Tip60 – – – + –
HA-KAT7 – – – – +
Flag-SMAD3 + + + + +
IP:Flag
Input
55
100
70
40
anti-Kinic
anti-Flag-SMAD3
anti-HA-hMOF/PCAF
Tip60/KAT7
anti-β-actin
B
HA-Tip60 – + ++
Flag-SMAD3 + + +
anti-HA-Tip60
C
si-Ctrl + – –
si-Tip60-1 – + –
si-Tip60-2 – – +
Flag-SMAD3 + + +
anti-Tip60
D
Ctrl + – –
TSA – + –
NAM – – +
Flag-SMAD3 + + +
E
HA-EV
HA-HDAC1
HA-HDAC2
HA-HDAC3
HA-HDAC4
HA-HDAC5
HA-HDAC6
HA-HDAC7
HA-HDAC8
HA-HDAC9
HA-HDAC10
Flag-SMAD3 + + + + + + + + + + +
anti-HA-HDAC1/2
anti-HA-HDAC3
anti-HA-HDAC4/5/6/
7/9
anti-HA-HDAC8
anti-HA-HDAC10
F
HA-HDAC6 – +
Flag-SMAD3 + +
INH + +
anti-HA-HDAC6
G
si-Ctrl + –
si-HDAC6 – +
Flag-SMAD3 + +
180
130
H
Flag-SMAD3 – +
HA-HDAC6 + +

**Figure 5. Tip60 and HDAC6 are the Kinic regulatory enzymes of SMAD3**

(A) Transfected with Flag-SMAD3 and 3×HA or HA-tagged hMOF, PCAF, Tip60, KAT7 for 48h, HEK293T cell lysates were subjected to IP with M2 beads, and then determined by Western blotting with indicated antibodies.

(B) Transfected with Flag-SMAD3 and co-transfected with concentration gradient HA-tagged Tip60 for 48h, HEK293T cell lysates were subjected to IP with M2 beads, and then determined by Western blotting with indicated antibodies.

(C) Transfected with Flag-SMAD3 after knockdown of Tip60 by siRNA, HEK293T cell lysates were subjected to IP with M2 beads, and then determined by Western blotting with indicated antibodies.

(D) Transfected with Flag-SMAD3 and treated with TSA and NAM, HEK293T cell lysates were subjected to IP with M2 beads, and then determined by Western blotting with indicated antibodies.

(E) Transfected with Flag-SMAD3 and HA-tagged HDAC1-10 for 48h, HEK293T cell lysates were subjected to IP with M2 beads, and then determined by Western blotting with indicated antibodies.

(F) Transfected with Flag-SMAD3 and HA-tagged HDAC6, HEK293T cell lysates were subjected to IP with M2 beads, and then determined by Western blotting with indicated antibodies.

(G) Transfected with Flag-SMAD3 after knockdown of HDAC6 by siRNA, HEK293T cell lysates were subjected to IP with M2 beads, and then determined by Western blotting with indicated antibodies.

(H) Transfected with Flag-SMAD3 and HA-HDAC6, HEK293T cell lysates were subjected to IP with M2 beads, and then determined by Western blotting with indicated antibodies.

liver cell THLE-2 and different liver cancer cells including LM3, HepG2, Huh7.5.1, SNU-739, and HCC9810 for endogenous Kinic analysis of SMAD3, and we found the Kinic level of SMAD3 was higher in LM3, HepG2, and Huh7.5.1 cells while lower in SNU739 and HCC9810 cells than THLE-2 cell (Figure S5A). This result indicated that Kinic of SMAD3 may has different functions in different liver cancer cells. To further investigate the function of SMAD3 Kinic, we detected the expression of TGFβ pathway downstream target and EMT-related genes following treatment with INH. Our findings revealed an increase in the expression levels of TGFβ pathway-associated downstream target genes such as *IL-22*, *CTGF*, *TNFα*, and *SMAD7*, while *SMAD3* expression remained unchanged (Figures 7A and S5B). These results suggest that INH treatment activates the TGFβ signaling pathway. Additionally, INH treatment led to the mRNA expression upregulation of EMT-related proteins N-cadherin, SLUG, and ZEB1, alongside a decrease in E-cadherin mRNA expression, indicating that INH treatment promoted EMT (Figures 7A and S5B). Consistent with changes in transcription levels, INH treatment increased N-cadherin protein expression and decreased E-cadherin levels (Figures 7B and S5C). Interestingly, phosphorylated-SMAD3 (*p*-SMAD3) (Ser423/425) levels also significantly increased following INH treatment (Figures 7B and S5C). Interestingly, knockdown of SMAD3 using siRNA resulted in decreased expression of EMT- or TGFβ pathway-associated genes and proteins following INH treatment (Figures 7C and S5D). These results suggest that INH induces activation of the TGFβ pathway and EMT by influencing SMAD3 protein rather than its gene transcription level. We further found that SMAD3(K378R) attenuates the promoting effect of downstream genes of the TGFβ pathway and EMT compared to SMAD3(WT) (Figure 7D). Immunofluorescence analysis and nuclear-cytoplasmic separation experiment were performed to explore the function of Kinic in this process. The results showed that INH increased Flag-SMAD3 (WT) levels in the nucleus; however, Flag-SMAD3 (K378R), which is insensitive to Kinic, showed no change in nuclear levels (Figures 7E and S5E). When considering the alteration in *p*-SMAD3 (Ser423/425) levels following INH treatment, this observation suggests that INH may promote SMAD3 Kinic, further phosphorylation, and subsequent nuclear translocation. Previous reports have highlighted that SMAD3 phosphorylation by TGFβ receptor I is essential for its translocation into the nucleus.[9] We found that TGFβ receptor I inhibitor SB431542 can effectively block SMAD3 transportation to the nucleus following INH treatment (Figures 7F and S6A). We found that INH strengthened the interaction between SMAD3, SMAD2/4, SARA, and KPNB1 in HepG2 and HeLa cells (Figures S6B and S6C). These results show that Kinic of SMAD3 promotes its phosphorylation and translocation into the nucleus, as well as downstream target genes expression.

We also found that treatment with INH significantly increased the migration, invasion, and clone formation abilities of HepG2 cells (Figures 8A and 8B). Furthermore, we overexpressed SMAD3 (WT) and SMAD3 (K378R) in HepG2 cells. The results indicated that overexpression of SMAD3 (WT) promoted HepG2 cell migration and invasion, whereas the SMAD3 (K378R) mutant attenuated this effect (Figure 8C). In conclusion, Kinic of SMAD3 promotes migration, invasion, and EMT in HepG2 cells.

## DISCUSSION

Since the 1960s, research into protein acylation modifications has flourished, with the initial discovery of histone acetylation's role in gene transcription regulation.[28,29] In the 1980s, the non-histone protein p53 was identified as being regulated by acetylation, marking the first instance of non-histone protein modification by acylation.[30] With the development of MS and new technologies, including PTMap, the study of protein acylation has undergone unprecedented development.[31] Recently, various novel short-chain protein acylation types have been identified, with histones and thousands of non-histone proteins identified as acylation targets.[6,32,33] In addition, almost all PTMs, as chemical regulatory factors of key molecules, govern protein function in various diseases by modifying epigenetic characteristics and cell signaling networks.[34,35]

Kinic, a novel type of histone acylations, was first identified in 2021.[8] According to the previous study, histone Kinic can be induced by the anti-tuberculosis drug INH or its downstream metabolites isonicotinic acid and promote tumor progression by activating the PI3K/AKT/mTOR signaling pathway. Although the previous report mentioned the possibility of non-histone proteins undergoing Kinic, the specific distribution patterns and functional implications of isonicotinylated non-histone proteins in mediating metabolic reprogramming during cancer progression remain poorly defined.[8] In this study, we identified 11,442 sites on 2,792 proteins capable of Kinic. Abundant isonicotinylated

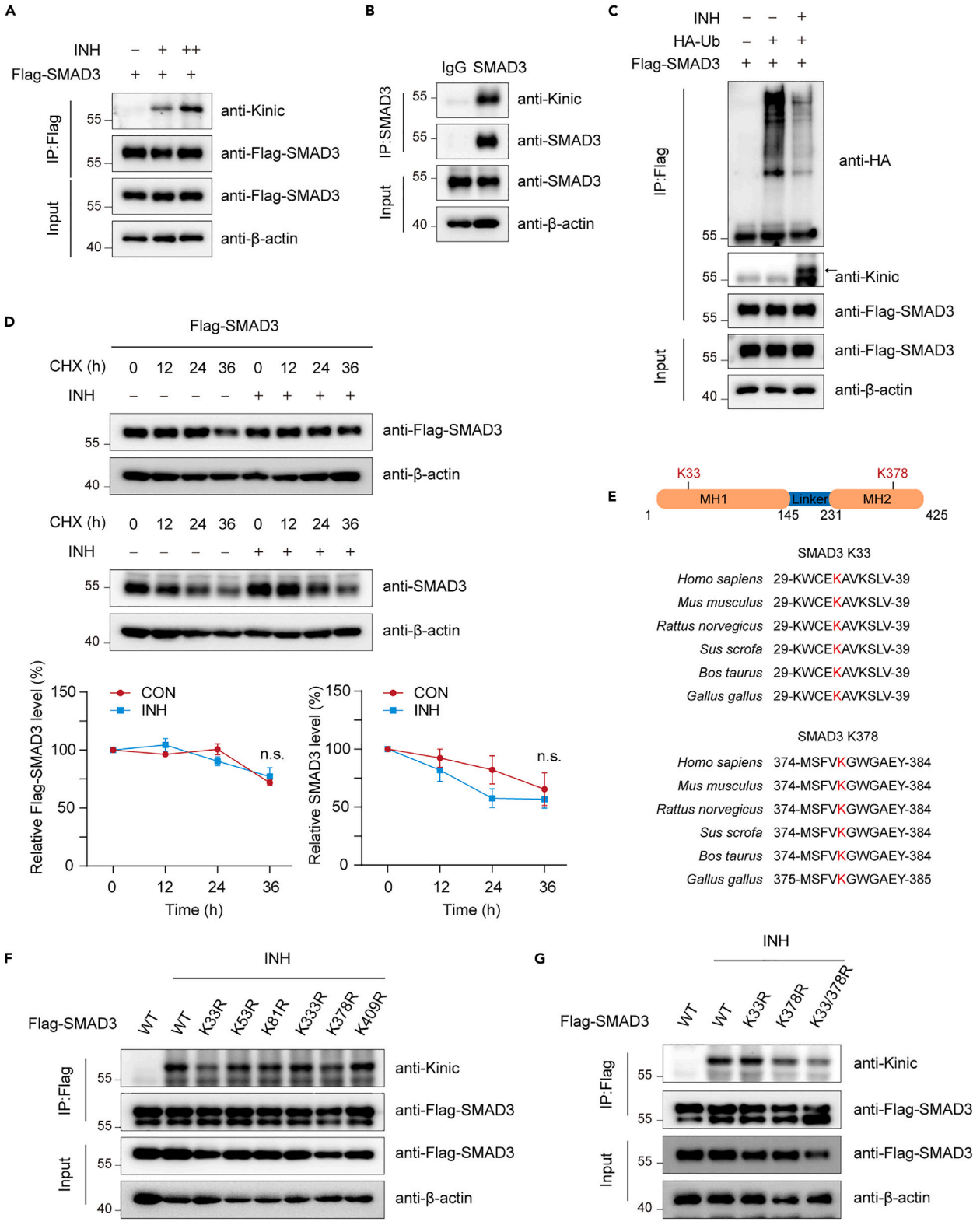


**Figure 6. K378 is the major Kinic site of SMAD3**

(A) HeLa cells transfected with FLAG-SMAD3 plasmids were treated with 0, 5, 10 mM INH for 24 h, and then cell lysates were subjected to IP with M2 beads, determined by Western blotting with indicated antibodies.

**Figure 6. *Continued***

(B) HeLa cells were treated with 10 mM INH for 24 h, and then cell lysates were subjected to IP with anti-SMAD3 antibody, determined by Western blotting with indicated antibodies.

(C) HeLa cells transfected with FLAG-SMAD3 and HA-Ub plasmids were treated with or without 10 mM INH for 24 h, and then cell lysates were subjected to IP with M2 beads, determined by Western blotting with indicated antibodies.

(D) HeLa cells transfected with or without FLAG-SMAD3 plasmids were treated with 10 mM INH and 100 mg/mL CHX treatment. Statistics of protein level stability in HeLa cells by ImageJ, as determined by two-way ANOVA test.

(E) The sequences surrounding K33 and K378 in SMAD3 among six species were aligned. Lysine (K) 33 and 378 of SMAD3 was colored in red.

(F–G). HeLa cells transfected with FLAG-SMAD3 mutant plasmids were treated with 10 mM (f) or 20 mM (g) of INH for 24 h, and then cell lysates were subjected to IP with M2 beads, determined by Western blotting with indicated antibodies.

non-histone proteins are extensively involved in various metabolic processes, including nucleocytoplasmic transport, carbon metabolism, the TCA cycle, amino acid biosynthesis, and oxidative phosphorylation. These results provide evidence for the physiological role of the dynamic Kinic of non-histones in metabolic regulation.

Regulatory enzymes involved in histone Kinic include isonicotinyl-transferases CBP/p300 and deisonicotinylase HDAC3.[8] Therefore, investigating the systems regulating non-histone Kinic is also crucial. The DNA damage factor PARP1 plays a critical role in double-strand break repair.[23,36–38] We demonstrated that Kinic of PARP1 is catalyzed by CBP and removal of isonicotinyl by HDAC8. These results also showed that Kinic may play a role in the DNA damage repair response. However, the specific functional role of the Kinic underlying DNA repair response requires further investigations.

Another protein of interest is SMAD3, involved in the TGFβ signaling pathway. The TGFβ signaling pathway governs processes such as embryo development, EMT, and injury repair through coordinated effects on cell proliferation, phenotypic plasticity, migration, and metabolic adaptation across multiple cell types.[39,40] In canonical signaling pathways, five ''receptor-regulated SMADs'' (R-SMADs) proteins, including SMAD2 and SMAD3, are phosphorylated by type I TGFβ receptors, whereas SMAD1, 5, and 8 are phosphorylated by BMP subfamily receptors.[41] After phosphorylation, R-SMAD-R-SMAD-SMAD4 trimeric complexes assemble and move into the nucleus, where they are involved in transcriptional regulation.[42] Notably, SMAD3 is the dominant molecule in this signaling pathway.[9] In the present study, we found that Tip60 is an isonicotinyl-transferase, whereas HDAC6 is a deisonicotinylase that regulates SMAD3 Kinic. Moreover, our research revealed the significance of SMAD3 Kinic in regulating EMT development in HepG2 and HeLa cells. INH treatment induces Kinic of SMAD3 at K378, facilitating its phosphorylation and nuclear accumulation. Consequently, Kinic of SMAD3 leads to increased transcriptional expression of downstream TGFβ and EMT-associated genes, as well as enhanced colony formation, migration, and invasion abilities of liver cancer cells. Therefore, Kinic of SMAD3 is beneficial for activating TGFβ and EMT signaling pathways (Figure 8D). These findings expand our understanding of SMAD3 functions and shed light on the role of SMAD3 Kinic in cancer metastasis.

INH has long been employed in the treatment of tuberculosis, but the underlying mechanism leading to an immune response and liver injury in certain patients remains a subject of controversy.[43] This study was prompted by the observation of Kinic of non-histones induced by INH, suggesting a potential role in the side effects associated with INH. Furthermore, when administering INH for tuberculosis treatment in the future, consideration of the risk posed by changes induced by non-histone Kinic, such as tumor promotion, becomes important.

In summary, our findings highlight that non-histone proteins are subject to Kinic, and these modifications may differ from those occurring on histone proteins. Notably, histone and non-histone Kinic involve distinct regulatory enzymes and functions. Simultaneously, these findings linking non-histone protein Kinic to tumors address the previously limited knowledge on Kinic of non-histone proteins. It is noteworthy that understanding non-histone protein Kinic enriches our comprehension of PTMs at the proteomic level, facilitating precise regulation of protein function.

### Limitations of the study

This study serves as an initial exploration of non-histone protein Kinic. Although regulatory systems for Kinic of SMAD3 and PARP1 have been identified, subsequent research on the Kinic of different proteins is crucial, including the effects on different non-histone proteins following Kinic in various metabolic pathways, the regulatory enzymes for different non-histone proteins, and the crosstalk between Kinic and other modifications. In addition, it is also important to explore the Kinic functions in different cells, which will help to understand the specificity in different cancer types and systematic diseases of this novel modification.

## RESOURCE AVAILABILITY

### Lead contact

Further information and requests for resources and reagents should be directed to and will be fulfilled by the lead contact, H.Z. (Hongquan.Zhang@bjmu.edu.cn).

### Materials availability

This study did not generate new unique reagents.

### Data and code availability

- The source data of MS proteomics have been deposited to the ProteomeXchange Consortium (http://proteomecentral.proteomexchange.org) via the PRIDE partner repository with the dataset identifier PXD050143 and PXD053507. The other data that support this study are available from the corresponding author upon reasonable request.

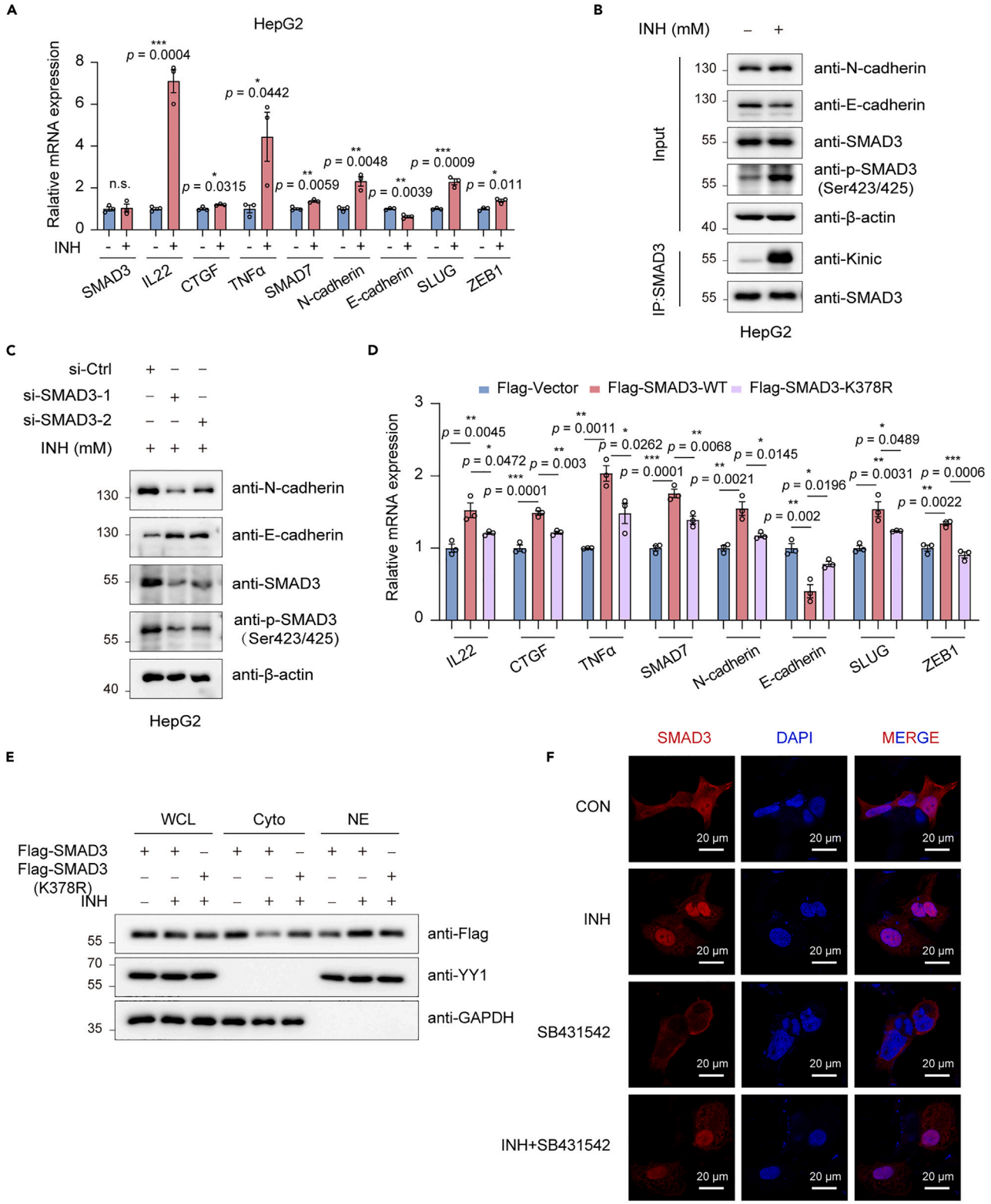


**Figure 7. Kinic of SMAD3 promoting phosphorylation, translocation into the nucleus and expression of EMT- or TGFβ pathway-associated genes**

(A) HepG2 cells were treated with 10 mM INH for 24 h, and then relevant genes level were determined by qPCR. Data are represented as mean ± SEM ($n = 3$), as determined by unpaired two-tailed Student's t test.

**Figure 7. *Continued***

(B) HepG2 cells were treated with 10 mM INH for 24 h, and then cell lysates tested by Western blotting using indicated antibodies.

(C) HepG2 cells were treated with 10 mM INH after treated with siRNA of SMAD3 for 24 h, and then cell lysates tested by Western blotting using related antibodies.

(D) HepG2 cells were transfected separately with Flag-Vector, Flag-SMAD3 (WT) and Flag-SMAD3 (K378R), and then relevant genes level were determined by qPCR. Data are represented as mean ± SEM ($n$ = 3), as determined by one-way ANOVA test.

(E) HepG2 cells transfected separately with Flag-SMAD3 (WT) or Flag-SMAD3 (K378R) were treated with or without 10 mM INH for 24 h and then cell lysates after nuclear-cytoplasmic separation were tested by Western blotting using indicated antibodies. WCL: whole cell lysate, Cyto: cytoplasmic, NE: nuclear.

(F) HepG2 cells were treated with 10 mM INH or 10 μM TGFβ receptor I inhibitor SB431542 for 24 h and stained with anti-SMAD3 antibodies, followed by visualization with confocal microscopy. Scale bar, 20μm.

- This article does not report original code.
- Any additional information required to reanalyze the data reported in this paper is available from the lead contact upon request.

## ACKNOWLEDGMENTS

This study was supported by grants from the Ministry of Science and Technology of China (grants 2022YFA1104003 and 2021YFC2501000) and National Natural Science Foundation of China (grants 82230094 and 81972616) to H.Z. National Natural Science Foundation of China (grant 82203325), Postdoctoral Research Foundation of China (grant 2022M710262) and National Postdoctoral Program for Innovative Talents of China (grant BX20220019) to Y.J.

## AUTHOR CONTRIBUTIONS

Y.L. and Y.J. designed the research, performed experiments, analyzed the data and wrote the manuscript. H.Y., Z.Q., and Y.P. constructed the plasmid. D.L. performed immunofluorescence experiments. H.Z. designed, supervised the research, and wrote the manuscript.

## DECLARATION OF INTERESTS

The authors declare no competing interests.

## STAR★METHODS

Detailed methods are provided in the online version of this paper and include the following:

- KEY RESOURCES TABLE
- EXPERIMENTAL MODEL AND STUDY PARTICIPANT DETAILS
  - Cell culture
- METHODS DETAILS
  - Reagents and antibodies
  - Plasmid constructs
  - HeLa cells extraction preparation and trypsin digestion
  - TMT labeling (for analysis of the cell kinic proteome)
  - Affinity enrichment
  - Liquid chromatography-tandem MS analysis
  - RNA interference
  - Western blotting and immunoprecipitation
  - Immunofluorescence
  - Quantitative polymerase chain reaction (qPCR)
  - Colony formation assay
  - Transwell assay
  - Bioinformatic analysis
- QUANTIFICATION AND STATISTICAL ANALYSIS

## SUPPLEMENTAL INFORMATION

Supplemental information can be found online at https://doi.org/10.1016/j.isci.2024.110775.

Received: April 11, 2024
Revised: July 2, 2024
Accepted: August 16, 2024
Published: August 21, 2024

## REFERENCES

1. Tan, M., Luo, H., Lee, S., Jin, F., Yang, J.S., Montellier, E., Buchou, T., Cheng, Z., Rousseaux, S., Rajagopal, N., et al. (2011). Identification of 67 Histone Marks and Histone Lysine Crotonylation as a New Type of Histone Modification. Cell *146*, 1016–1028. https://doi.org/10.1016/j.cell.2011.08.008.

2. Zhang, Z., Tan, M., Xie, Z., Dai, L., Chen, Y., and Zhao, Y. (2011). Identification of lysine succinylation as a new post-translational modification. Nat. Chem. Biol. *7*, 58–63. https://doi.org/10.1038/Nchembio.495.

3. Gao, Y., Sheng, X., Tan, D., Kim, S., Choi, S., Paudel, S., Lee, T., Yan, C., Tan, M., Kim, K.M., et al. (2023). Identification of Histone Lysine Acetoacetylation as a Dynamic Post-Translational Modification Regulated by HBO1. Adv. Sci. *10*, e2300032. https://doi.org/10.1002/advs.202300032.

4. Zhang, D., Tang, Z., Huang, H., Zhou, G., Cui, C., Weng, Y., Liu, W., Kim, S., Lee, S.,

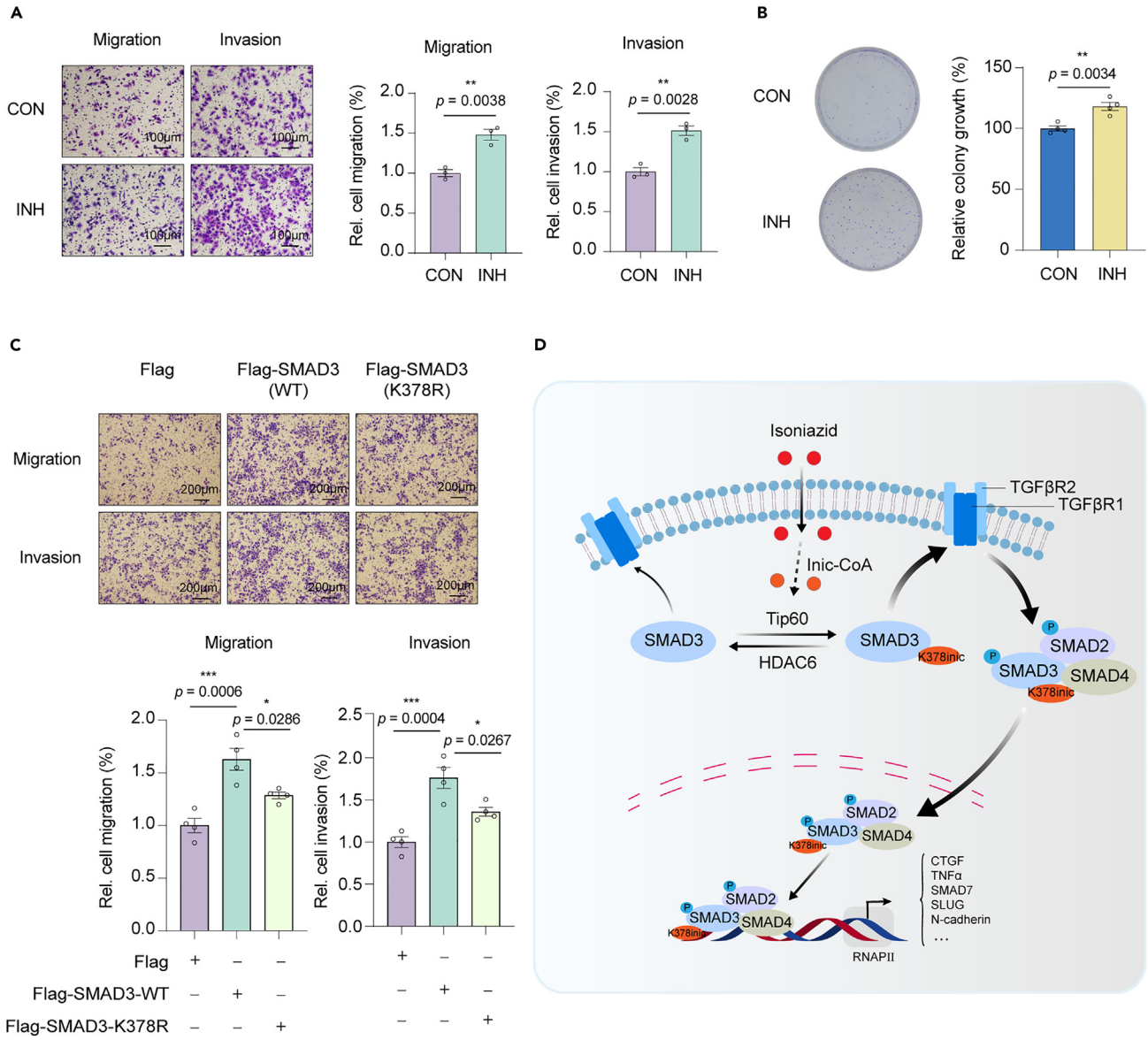


**Figure 8. K378inic is required for SMAD3 promoting liver cancer cell migration, invasion and EMT**

(A) HepG2 cells were treated with or without 10 mM INH and transwell assay was carried out to determine the migration and invasion ability. Data are represented as mean ± SEM ($n$ = 3), as determined by unpaired two-tailed Student's t test. Scale bar, 100 μm.

(B) HepG2 cells were treated with or without 10 mM INH and colony formation assay was carried out to determine forming ability. Data are represented as mean ± SEM ($n$ = 4), as determined by unpaired two-tailed Student's t test.

(C) HepG2 cells were transfected Flag-SMAD3 (WT) or Flag-SMAD3 (K378R) and transwell assay was carried out to determine the migration and invasion ability. Data are represented as mean ± SEM ($n$ = 4), as determined by one-way ANOVA test. Scale bar, 200μm.

(D) The working model of SMAD3 Kinic in TGFβ pathway in cellular.

Perez-Neut, M., et al. (2019). Metabolic regulation of gene expression by histone lactylation. Nature *574*, 575–580. https://doi.org/10.1038/s41586-019-1678-1.

5. Narita, T., Weinert, B.T., and Choudhary, C. (2019). Functions and mechanisms of non-histone protein acetylation. Nat Rev Mol Cell Bio *20*, 156–174. https://doi.org/10.1038/s41580-018-0081-3.
6. Sabari, B.R., Zhang, D., Allis, C.D., and Zhao, Y. (2017). Metabolic regulation of gene expression through histone acylations. Nat Rev Mol Cell Bio *18*, 90–101. https://doi.org/10.1038/nrm.2016.140.
7. Fu, Y., Yu, J., Li, F., and Ge, S. (2022). Oncometabolites drive tumorigenesis by enhancing protein acylation: from chromosomal remodelling to nonhistone modification. J Exp Clin Canc Res *41*, 144. https://doi.org/10.1186/s13046-022-02338-w.
8. Jiang, Y., Li, Y., Liu, C., Zhang, L., Lv, D., Weng, Y., Cheng, Z., Chen, X., Zhan, J., and Zhang, H. (2021). Isonicotinylation is a histone mark induced by the anti-tuberculosis first-line drug isoniazid. Nat. Commun. *12*, 5548. https://doi.org/10.1038/s41467-021-25867-y.
9. Massagué, J., and Sheppard, D. (2023). TGF-β signaling in health and disease. Cell *186*, 4007–4037. https://doi.org/10.1016/j.cell.2023.07.036.

10. Roberts, A.B., Tian, F., Byfield, S.D., Stuelten, C., Ooshima, A., Saika, S., and Flanders, K.C. (2006). Smad3 is key to TGF-beta-mediated epithelial-to-mesenchymal transition, fibrosis, tumor suppression and metastasis. Cytokine Growth Factor Rev. *17*, 19–27. https://doi.org/10.1016/j.cytogfr.2005.09.008.
11. Meng, X.M., Nikolic-Paterson, D.J., and Lan, H.Y. (2016). TGF-β: the master regulator of fibrosis. Nat. Rev. Nephrol. *12*, 325–338. https://doi.org/10.1038/nrneph.2016.48.
12. Shi, Y., and Massagué, J. (2003). Mechanisms of TGF-β signaling from cell membrane to the nucleus. Cell *113*, 685–700. https://doi.org/10.1016/S0092-8674(03)00432-X.
13. Miyazawa, K., and Miyazono, K. (2017). Regulation of TGF-β Family Signaling by Inhibitory Smads. Cold Spring Harb. Perspect. Biol. *9*, a022095. https://doi.org/10.1101/cshperspect.a022095.
14. Huang, C., Hu, F., Song, D., Sun, X., Liu, A., Wu, Q., She, X., Chen, Y., Chen, L., Hu, F., et al. (2022). EZH2-triggered methylation of promotes its activation and tumor metastasis. J. Clin. Invest. *132*, e152394. https://doi.org/10.1172/JCI152394.
15. Yu, B., Luo, F., Sun, B., Liu, W., Shi, Q., Cheng, S.Y., Chen, C., Chen, G., Li, Y., and Feng, H. (2022). KAT6A Acetylation of SMAD3 Regulates Myeloid-Derived Suppressor Cell Recruitment, Metastasis, and Immunotherapy in Triple-Negative Breast Cancer. Adv. Sci. *9*, e2105793. https://doi.org/10.1002/advs.202105793.
16. Gao, S., Alarcón, C., Sapkota, G., Rahman, S., Chen, P.Y., Goerner, N., Macias, M.J., Erdjument-Bromage, H., Tempst, P., and Massagué, J. (2009). Ubiquitin Ligase Nedd4L Targets Activated Smad2/3 to Limit TGF-β Signaling. Mol. Cell *36*, 457–468. https://doi.org/10.1016/j.molcel.2009.09.043.
17. Li, K., Zhang, T.T., Wang, F., Cui, B., Zhao, C.X., Yu, J.J., Lv, X.X., Zhang, X.W., Yang, Z.N., Huang, B., et al. (2018). Metformin suppresses melanoma progression by inhibiting KAT5-mediated SMAD3 acetylation, transcriptional activity and TRIB3 expression. Oncogene *37*, 2967–2981. https://doi.org/10.1038/s41388-018-0172-9.
18. Yuan, Y., Li, Y., Wu, X., Bo, J., Zhang, L., Zhang, J., Hu, Y., Chen, Y., Zeng, Y., Wei, X., and Zhang, H. (2024). POH1 induces Smad3 deubiquitination and promotes lung cancer metastasis. Cancer Lett. *582*, 216526. https://doi.org/10.1016/j.canlet.2023.216526.
19. Weinert, B.T., Schölz, C., Wagner, S.A., Iesmantavicius, V., Su, D., Daniel, J.A., and Choudhary, C. (2013). Lysine Succinylation Is a Frequently Occurring Modification in Prokaryotes and Eukaryotes and Extensively Overlaps with Acetylation. Cell Rep. *4*, 842–851. https://doi.org/10.1016/j.celrep.2013.07.024.
20. Yuan, Y., Yuan, H., Yang, G., Yun, H., Zhao, M., Liu, Z., Zhao, L., Geng, Y., Liu, L., Wang, J., et al. (2020). IFN-alpha confers epigenetic regulation of HBV cccDNA minichromosome by modulating GCN5-mediated succinylation of histone H3K79 to clear HBV cccDNA. Clin. Epigenetics *12*, 135. https://doi.org/10.1186/s13148-020-00928-z.
21. Koronowski, K.B., Greco, C.M., Huang, H., Kim, J.K., Fribourgh, J.L., Crosby, P., Mathur, L., Ren, X., Partch, C.L., Jang, C., et al. (2021). Ketogenesis impact on liver metabolism revealed by proteomics of lysine β-hydroxybutyrylation. Cell Rep. *36*, 109487. https://doi.org/10.1016/j.celrep.2021.109487.
22. Jackson, S.P., and Bartek, J. (2009). The DNA-damage response in human biology and disease. Nature *461*, 1071–1078. https://doi.org/10.1038/nature08467.
23. Scully, R., Panday, A., Elango, R., and Willis, N.A. (2019). DNA double-strand break repair-pathway choice in somatic mammalian cells. Nat. Rev. Mol. Cell Bio. *20*, 698–714. https://doi.org/10.1038/s41580-019-0152-0.
24. Inui, M., Manfrin, A., Mamidi, A., Martello, G., Morsut, L., Soligo, S., Enzo, E., Moro, S., Polo, S., Dupont, S., et al. (2011). USP15 is a deubiquitylating enzyme for receptor-activated SMADs. Nat. Cell Biol. *13*, 1368–1375. https://doi.org/10.1038/ncb2346.
25. Tang, L.Y., Yamashita, M., Coussens, N.P., Tang, Y., Wang, X., Li, C., Deng, C.X., Cheng, S.Y., and Zhang, Y.E. (2011). Ablation of Smurf2 reveals an inhibition in TGF-β signalling through multiple mono-ubiquitination of Smad3. EMBO J. *30*, 4777–4789. https://doi.org/10.1038/emboj.2011.393.
26. Zhao, X.Y., Chen, J.Y., Sun, H.X., Zhang, Y., and Zou, D.W. (2022). New insights into fibrosis from the ECM degradation perspective: the macrophage-MMP-ECM interaction. Cell Biosci. *12*, 117. https://doi.org/10.1186/s13578-022-00881-9.
27. Zou, M.L., Chen, Z.H., Teng, Y.Y., Liu, S.Y., Jia, Y., Zhang, K.W., Sun, Z.L., Wu, J.J., Yuan, Z.D., Feng, Y., et al. (2021). The Smad Dependent TGF-β and BMP Signaling Pathway in Bone Remodeling and Therapies. Front. Mol. Biosci. *8*, 593310. https://doi.org/10.3389/fmolb.2021.593310.
28. Phillips, D.M. (1963). The presence of acetyl groups of histones. Biochem. J. *87*, 258–263. https://doi.org/10.1042/bj0870258.
29. Verdin, E., and Ott, M. (2015). 50 years of protein acetylation: from gene regulation to epigenetics, metabolism and beyond. Nat Rev Mol Cell Bio *16*, 258–264. https://doi.org/10.1038/nrm3931.
30. Gu, W., and Roeder, R.G. (1997). Activation of p53 sequence-specific DNA binding by acetylation of the p53 C-terminal domain. Cell *90*, 595–606. https://doi.org/10.1016/S0092-8674(00)80521-8.
31. Chen, Y., Chen, W., Cobb, M.H., and Zhao, Y. (2009). PTMap–a sequence alignment software for unrestricted, accurate, and full-spectrum identification of post-translational modification sites. Proc. Natl. Acad. Sci. USA *106*, 761–766. https://doi.org/10.1073/pnas.0811739106.
32. Shvedunova, M., and Akhtar, A. (2022). Modulation of cellular processes by histone and non-histone protein acetylation. Nat Rev Mol Cell Bio *23*, 329–349. https://doi.org/10.1038/s41580-021-00441-y.
33. Xu, Y., Shi, Z., and Bao, L. (2022). An Expanding Repertoire of Protein Acylations. Mol. Cell. Proteomics *21*, 100193. https://doi.org/10.1016/j.mcpro.2022.100193.
34. Deribe, Y.L., Pawson, T., and Dikic, I. (2010). Post-translational modifications in signal integration. Nat. Struct. Mol. Biol. *17*, 666–672. https://doi.org/10.1038/nsmb.1842.
35. Dutta, A., Abmayr, S.M., and Workman, J.L. (2016). Diverse Activities of Histone Acylations Connect Metabolism to Chromatin Function. Mol. Cell *63*, 547–552. https://doi.org/10.1016/j.molcel.2016.06.038.
36. Ciccia, A., and Elledge, S.J. (2010). The DNA Damage Response: Making It Safe to Play with Knives. Mol. Cell *40*, 179–204. https://doi.org/10.1016/j.molcel.2010.09.019.
37. Izhar, L., Adamson, B., Ciccia, A., Lewis, J., Pontano-Vaites, L., Leng, Y., Liang, A.C., Westbrook, T.F., Harper, J.W., and Elledge, S.J. (2015). A Systematic Analysis of Factors Localized to Damaged Chromatin Reveals PARP-Dependent Recruitment of Transcription Factors. Cell Rep. *11*, 1486–1500. https://doi.org/10.1016/j.celrep.2015.04.053.
38. Langelier, M.F., Planck, J.L., Roy, S., and Pascal, J.M. (2012). Structural Basis for DNA Damage-Dependent Poly(ADP-ribosyl)ation by Human PARP-1. Science *336*, 728–732. https://doi.org/10.1126/science.1216338.
39. Wu, M., Wu, S., Chen, W., and Li, Y.P. (2024). The roles and regulatory mechanisms of TGF-β and BMP signaling in bone and cartilage development, homeostasis and disease. Cell Res. *34*, 101–123. https://doi.org/10.1038/s41422-023-00918-9.
40. Moses, H.L., Roberts, A.B., and Derynck, R. (2016). The Discovery and Early Days of TGF-β: A Historical Perspective. Cold Spring Harb. Perspect. Biol. *8*, a021865. https://doi.org/10.1101/cshperspect.a021865.
41. Macias, M.J., Martin-Malpartida, P., and Massagué, J. (2015). Structural determinants of Smad function in TGF-β signaling. Trends Biochem. Sci. *40*, 296–308. https://doi.org/10.1016/j.tibs.2015.03.012.
42. Alarcón, C., Zaromytidou, A.I., Xi, Q., Gao, S., Yu, J., Fujisawa, S., Barlas, A., Miller, A.N., Manova-Todorova, K., Macias, M.J., et al. (2009). Nuclear CDKs Drive Smad Transcriptional Activation and Turnover in BMP and TGF-β Pathways. Cell *139*, 757–769. https://doi.org/10.1016/j.cell.2009.09.035.
43. Metushi, I., Uetrecht, J., and Phillips, E. (2016). Mechanism of isoniazid-induced hepatotoxicity: then and now. Br. J. Clin. Pharmacol. *81*, 1030–1036. https://doi.org/10.1111/bcp.12885.
44. Jin, J., Zhang, L., Li, X., Xu, W., Yang, S., Song, J., Zhang, W., Zhan, J., Luo, J., and Zhang, H. (2022). Oxidative stress-CBP axis modulates MOB1 acetylation and activates the Hippo signaling pathway. Nucleic Acids Res. *50*, 3817–3834. https://doi.org/10.1093/nar/gkac189.

## STAR★METHODS

### KEY RESOURCES TABLE

| REAGENT or RESOURCE | SOURCE | IDENTIFIER |
|---|---|---|
| Antibodies | | |
| Mouse monoclonal anti-Flag tag | Cell Signaling Technology | Cat#8146; RRID: AB_10950495 |
| Rabbit monoclonal anti-HA tag | Cell Signaling Technology | Cat#3724; RRID: AB_1549585 |
| Rabbit monoclonal anti-SMAD3 | Cell Signaling Technology | Cat#9523; RRID: AB_2193182 |
| Rabbit monoclonal anti-Phospho-SMAD3(Ser423/425) | Cell Signaling Technology | Cat#9520; RRID: AB_2193207 |
| Rabbit monoclonal anti-E-Cadherin | Cell Signaling Technology | Cat#3195; RRID: AB_2291471 |
| Mouse monoclonal anti-N-Cadherin | Cell Signaling Technology | Cat#14215; RRID: AB_2798427 |
| Rabbit monoclonal anti-CBP | Cell Signaling Technology | Cat#7389; RRID: AB_2616020 |
| Rabbit monoclonal anti-HDAC6 | Cell Signaling Technology | Cat#7558; RRID: AB_10891804 |
| Rabbit monoclonal anti-HDAC8 | Cell Signaling Technology | Cat#66042; RRID: AB_2895217 |
| Mouse monoclonal anti-TIP60 | HUABIO | Cat#EM1706-52; |
| Rabbit monoclonal anti-ACTN4 | HUABIO | Cat#ET1706-05; RRID: AB_3070631 |
| Mouse monoclonal anti-β-actin | ABMART | Cat#T40104F; RRID: AB_2936320 |
| Mouse monoclonal anti-Talin | Merck Millipore | Cat#05–1144; RRID: AB_10628001 |
| Mouse monoclonal anti-Ezrin | Abcam | Cat#ab4069; RRID: AB_304261 |
| Rabbit anti-pan-Kinic | PTM BIO | N/A; Customized |
| Bacterial and virus strains | | |
| DH5α Competent Cells | TIANGEN | Cat#CB101 |
| Chemicals, peptides, and recombinant proteins | | |
| Isoniazid | Sigma-Aldrich | Cat#I3377 |
| Cycloheximide | Sigma-Aldrich | Cat#C7698 |
| Trichostatin A | MedChemExpress | Cat#HY-15144 |
| Nicotinamide | MedChemExpress | Cat# HY-B0150 |
| SGC-CBP30 | MedChemExpress | Cat#HY-15826 |
| A-485 | MedChemExpress | Cat#HY-107455 |
| BG45 | Selleck | Cat#S7689 |
| MC1568 | Selleck | Cat#S1484 |
| CAY10603 | Selleck | Cat#S7596 |
| JNJ-26481585 | Selleck | Cat#S1096 |
| NaBu | Aladdin | Cat#S102954 |
| Anti-Flag Affinity Gel | YEASEN | Cat#20584ES08 |
| Protease inhibitor cocktail | YEASEN | Cat#20123ES10 |
| Phosphatase inhibitor cocktail | YEASEN | Cat#20109ES05 |
| Hieff Trans® Liposomal Transfection Reagent | YEASEN | Cat#40802ES |
| Critical commercial assays | | |
| Transwell cell | Corning | Cat#CLS3422 |
| Matrigel Matrix | Corning | Cat#356231 |
| Hifair® III 1st Strand cDNA Synthesis SuperMix | YEASEN | Cat#11141ES |
| Hieff® qPCR SYBR Green Master Mix | YEASEN | Cat#11201ES |
| Nuclear and cytoplasmic protein extraction kit | Beyotime | Cat#P0028 |

(*Continued on next page*)

*Continued*

| REAGENT or RESOURCE | SOURCE | IDENTIFIER |
|---|---|---|
| Deposited data | | |
| LC-MS/MS data | This paper | PRIDE: PXD050143 |
| LC-MS/MS data | This paper | PRIDE: PXD053507 |
| Experimental models: cell lines | | |
| Human: HEK293T | ATCC | ATCC CRL-3216 |
| Human: HeLa | ATCC | ATCC CCL-2 |
| Human: HepG2 | ATCC | ATCC HB-8065; |
| Oligonucleotides | | |
| siRNA-Ctrl: 5′-UUCUCCGAACGUGUCACGUTT-3′ | This paper | N/A |
| siRNA-CBP: 5′-AACAGTGGGAACCTTGTTCCA-3′ | This paper | N/A |
| siRNA-HDAC8: 5′-GGCCACCUUCCACACUGAUGCUUAU-3′ | This paper | N/A |
| siRNA-Tip60 #1: 5′-GAGAAAGAATCAACGGAAG-3′ | This paper | N/A |
| siRNA-Tip60 #2: 5′-TCGAATTGTTTGGGCACTGAT-3′ | This paper | N/A |
| siRNA-HDAC6: 5′-CTGCAAGGGATGGATCTGA-3′ | This paper | N/A |
| siRNA-SMAD3 #1: 5′-GCGUGAAUCCCUACCACUATT-3′ | This paper | N/A |
| siRNA-SMAD3 #2: 5′-GCCAUCCAUGACUGUGGAUTT-3′ | This paper | N/A |
| Primers for qPCR | Table S3 | N/A |
| Recombinant DNA | | |
| pcDNA3.1-FLAG-Vector | This paper | N/A |
| pcDNA3.1-FLAG-SMAD3 | This paper | N/A |
| pcDNA3.1-FLAG-SMAD3(K378R) | This paper | N/A |
| pcDNA3.1-FLAG-PARP1 | This paper | N/A |
| pcDNA3.1-FLAG-vigilin | This paper | N/A |
| pcDNA3.1-FLAG-FRMD8 | This paper | N/A |
| pcDNA3.1-FLAG-NPM1 | This paper | N/A |
| pcDNA3.1-FLAG-FSCN1 | This paper | N/A |
| pcDNA3.1-FLAG-MSN | This paper | N/A |
| pcDNA3.1-FLAG-FHL1 | This paper | N/A |
| pcDNA3.1-FLAG-HDAC1 | This paper | N/A |
| pcDNA3.1-FLAG-HDAC2 | This paper | N/A |
| pcDNA3.1-FLAG-ACLY | This paper | N/A |
| Software and algorithms | | |
| GraphPad Prism v8.0.2 | GraphPad | https://www.graphpad.com/ |
| ImageJ v1.8.0 | National Institutes of Health | National Institutes of Health |
| Maxquant v.1.5.2.8 | Maxquant | https://www.maxquant.org/ |
| Wolfpsort v.0.2 | Wolfpsort Software | https://wolfpsort.hgc.jp/ |

## EXPERIMENTAL MODEL AND STUDY PARTICIPANT DETAILS

### Cell culture

HEK293T, HeLa, HepG2 cell lines were originally obtained from ATCC. All cell lines were maintained in DMEM supplemented with 10% fetal bovine serum (FBS) and 100 U/mL penicillin and 100 U/mL streptomycin. All cells were maintained at 37°C in a saturated humidity atmosphere containing 5% $CO_2$.

## METHODS DETAILS

### Reagents and antibodies

Isoniazid (I3377) and Cycloheximide (CHX, C7698) were purchased from Sigma-Aldrich. Trichostatin A (TSA, HY-15144), Nicotinamide (NAM, HY-B0150), SGC-CBP30 (HY-15826), and A-485 (HY-107455) were purchased from MedChemExpress. BG45 (S7689), MC1568 (S1484), CAY10603 (S7596), and JNJ-26481585 (S1096) were purchased from Selleck. NaBu (S102954) was purchased from Aladdin. Anti-Flag Affinity Gel (M2 beads, 20584ES08), protease inhibitor cocktail (20123ES10), and phosphatase inhibitor cocktail (20109ES05) were purchased from YEASEN. Transwell (CLS3422) and Matrigel Matrix (356231) were purchased from Corning. Hifair III 1st Strand cDNA Synthesis SuperMix (11141ES) and Hieff qPCR SYBR Green Master Mix (11201ES) for qPCR were purchased from YEASEN. Rabbit-*anti*-pan-Kinic antibody (1:1000 for WB) was designed and prepared by PTM Biolabs Inc. Mouse-*anti*-Flag (#8146, 1:6000 for WB, 1:300 for IF), rabbit-*anti*-HA (#3724, 1:6000 for WB, 1:300 for IF), rabbit-*anti*-SMAD3 (#9523, 1:1000 for WB, 1:200 for IF), rabbit-*anti*-phospho-SMAD3 (Ser423/425) (#9520, 1:1000 for WB), rabbit-*anti*-E-cadherin (#3195, 1:1000 for WB), mouse-*anti*-N-cadherin (#14215, 1:1000 for WB), rabbit-*anti*-CBP (#7389, 1:1000 for WB), rabbit-*anti*-HDAC6 (#7558, 1:1000 for WB), rabbit-*anti*-HDAC8 (#66042, 1:1000 for WB) were purchased from Cell Signaling Technology. Mouse-*anti*-Tip60 (#EM1706-52, 1:1000 for WB) and mouse-*anti*-ACTN4 (#Et17065, 1:6000 for WB) were purchased from HUABIO. Mouse-*anti*-β-actin (#T40104F, 1:6000 for WB) was purchased from ABMART. Mouse-*anti*-Talin (#05–1144, 1:1000 for WB) was purchased from Merck Millipore. Mouse-*anti*-Ezrin (#ab4069, 1:1000 for WB) was purchased from Abcam.

### Plasmid constructs

All plasmids including acetyltransferase and deacetyltransferases were indicated in our previous publication.[44] FLAG-tagged PARP1 was a generous gift from by Dr. Jiadong Wang (Peking University Health Science Center, Beijing, China). The FLAG-SMAD3 mutants were constructed using wild-type SMAD3 as template with Fast Site-Directed Mutagenesis Kit (TIANGEN, KM101).

### HeLa cells extraction preparation and trypsin digestion

HeLa cells were treated with 10 mM INH for 24 h and sonicated on ice using a high intensity ultrasonic processor in lysis buffer (8 M urea, 3 μM TSA and 50 mM NAM, 1% protease inhibitor cocktail). After centrifugation at 12000*g* and 4°C for 10 min, the supernatant was collected, the protein concentration was determined. For trypsin digestion, 5 mM dithiothreitol was used to reduce protein solution for 30 min at 56°C and 11 mM iodoacetamide was used to alkylate protein for 15 min at room temperature in darkness. 100 mM triethylammonium bicarbonate (TEAB) was added to dilute protein sample. Then, 1:50 trypsin-to-protein mass ratio trypsin digestion was performed for the first overnight and 1:100 trypsin-to-protein mass ratio digestion for a second 4 h digestion.

### TMT labeling (for analysis of the cell kinic proteome)

Tryptic peptides were dissolved in 0.5 M TEAB and processed according to the manufacturer's protocol for TMT kit. Briefly, one unit of TMT reagent were thawed and reconstituted in acetonitrile. The peptide mixtures were pooled, desalted and dried by vacuum centrifugation after incubated for 2 h at room temperature. Next, the samples were fractionated by high-pH reversed-phase high-performance liquid chromatography (HPLC) using Thermo Betasil C18 column (5 μm particles, 10 mm ID, 250 mm length).

### Affinity enrichment

To enrich Kinic modified peptides, tryptic peptides dissolved in NETN buffer (100 mM NaCl, 1 mM EDTA, 50 mM Tris-HCl, 0.5% NP-40, pH 8.0) were incubated with prewashed antibody beads (PTM Biolab Co. Ltd.) at 4°C overnight with gentle shaking. Then, the beads were washed four times with NETN buffer and twice with $H_2O$. The bound peptides were eluted from the beads with 0.1% trifluoroacetic acid. Finally, the eluted fractions were combined and vacuum-dried. The resulting peptides were desalted with C18 ZipTips (ZTC18S960, Millipore) according to the manufacturer's instructions.

### Liquid chromatography-tandem MS analysis

The enriched isonicotinylated peptides were dissolved in 0.1% formic acid (solvent A), directly loaded onto a home-made reversed phase analytical column (15 cm length, 75 μm). The gradient comprised an increasing from 7% to 23% solvent B (0.1% formic acid in 98% acetonitrile) over 24 min, 23%–35% in 8 min, and increasing to 80% over 4 min then holding at 80% for the last 4 min, all at a constant flow rate of 500 nL/min on an EASY-nLC 1200 UPLC system. The separated peptides were subjected to the NSI source followed by tandem mass spectrometry (MS/MS) in HF-X (Thermo) coupled online to the UPLC. The electrospray voltage was 2.1 kV. The full MS scan resolution was set to 120,000 over a scan range of 350–1600 m/z. Peptides were then selected for MS/MS using NCE setting as 28% and the fragment ions were detected in the Orbitrap at a resolution of 15,000. A data-dependent procedure alternated between one MS scan and 20 MS/MS scans with 10.0 s dynamic exclusion. Automatic gain control (AGC) was set at 1E5. Fixed first mass was set as 100 m/z.

### RNA interference

Small interfere RNA was used for knockdown of proteins level. The sequences of siRNA for target genes as follows:

siCtrl: 5′-UUCUCCGAACGUGUCACGUTT-3′;
siCBP: 5′-AACAGTGGGAACCTTGTTCCA-3′;
siHDAC8: 5′-GGCCACCUUCCACACUGAUGCUUAU-3′;
siTip60#1: 5′-GAGAAAGAATCAACGGAAG-3′;
siTip60#2: 5′-TCGAATTGTTTGGGCACTGAT-3′;
siHDAC6: 5′-CTGCAAGGGATGGATCTGA-3′;
siSMAD3#1: 5′-GCGUGAAUCCCUACCACUATT-3′;
siSMAD3#2: 5′-GCCAUCCAUGACUGUGGAUTT-3′; All the above siRNA oligos were synthesized from TSINGKE. The siRNAs were used to transfect cells by using Hieff Trans Liposomal Transfection Reagent (40802ES) purchased from YEASEN.

### Western blotting and immunoprecipitation

Cells were lysed with RIPA buffer (50 mM Tris-HCL pH 8.0, 150 mM NaCl, 1% Triton X-100, 0.1% SDS, 1 mM EDTA, 1% sodium deoxycholic acid, protease inhibitor, and phosphatase inhibitor) on ice for 30 min after washed by PBS. For Western blotting, supernatant was collected by centrifugation and the concentration of protein was measured using Bicinchoninic acid (BCA) kit. SDS-PAGE experiment was carried out to transfer the protein to PVDF membranes and then the membranes were incubated with the indicated antibodies overnight after blocked in 5% skim milk for 1 h. For immunoprecipitation assay, after supernatant was collected, add same species primary antibodies and protein A/G agarose beads incubated overnight. Next day, after washing beads for 3 times using PBS, proteins were stripped with loading buffer. Supernatant was collected by centrifugation and the following steps are same as Western blotting. Nuclear and cytoplasmic protein extraction kits (P0028) were purchased from Beyotime Biotechnology and following the kit instructions to separate cell components.

### Immunofluorescence

Cells were fixed with 4% paraformaldehyde for 10 min, and permeabilized with PBS containing 0.1% Triton X-100 for 15 min. After blocked with 5% BSA for 1 h, cells were incubated with the indicated antibodies overnight at 4°C. Next day after washed and incubated with secondary antibodies (Alexa Flour 594 or 488, dilution 1:200), the cell nuclei were stained with DAPI. Images were captured with ALSM-780 616 confocal laser-scanning microscope (with Zeiss confocal Zen Software (v2011)).

### Quantitative polymerase chain reaction (qPCR)

Total RNA was isolated from samples with TRIzol reagents. cDNA was prepared with the Hifair III 1st Strand cDNA Synthesis SuperMix. Hieff qPCR SYBR Green Master Mix was used to quantitative PCR experiment. Expression level of GAPDH as the internal parameter. The sequences of primers for target genes are as follows:

*SMAD3*-F: 5′-TGGACGCAGGTTCTCCAAAC-3′;
*SMAD3*-R: 5′-CCGGCTCGCAGTAGGTAAC-3′;
*E-cadherin*-F: 5′-CTGATGCTGATGCCCCCAATA-3′;
*E-cadherin*-R: 5′-CAGTTTCTGCATCTTGCCAGG-3′;
*N-cadherin*-F: 5′-AGCCAACCTTAACTGAGGAGT-3′;
*N-cadherin*-R: 5′-GGCAAGTTGATTGGAGGGATG-3′;
*IL22*-F: 5′-GACAAGTCCAACTTCCAG-3′;
*IL22*-R: 5′-GCTCACTCATACTGACTC-3′;
*CTGF*-F: 5′-CTGTGGAGTATGTACCGACGGCC-3′;
*CTGF*-R: 5′-ATGGCAGGCACAGGTCTTGATGAAC-3′;
*TNFα*-F: 5′-TGCACTTTGGAGTGATCGGC-3′;
*TNFα*-R: 5′-CTCAGCTTGAGGGTTTGCTAC-3′;
*SMAD7*-F: 5′-TTCCTCCGCTGAAACAGGG-3′;
*SMAD7*-R: 5′-CCTCCCAGTATGCCACCAC-3′;
*SLUG*-F: 5′-CGAACTGGACACACATACAGTG-3′;
*SLUG*-R: 5′-CTGAGGATCTCTGGTTGTGGT-3′;
*ZEB1*-F: 5′-TGCACTGAGTGTGGAAAAGC-3′;
*ZEB1*-R: 5′-TGGTGATGCTGAAAGAGACG-3′.

### Colony formation assay

Total $1\times10^3$ HepG2 cells per group were seeded in 6-well plates and cultured with or without 10 mM INH treatment for 10 days. The cells fixed with 4% paraformaldehyde for 30 min were stained with 0.1% crystal violet solution and photographed. 30% of acetic acid was used to extract crystal violet from plates. Relative growth was quantified by OD value.

### Transwell assay

Before experiment, HepG2 cells were transfected with Flag-SMAD3 (WT) or Flag-SMAD3 (K378R). The upper chamber is covered with a layer of matrix gel in invasion assay. $3 \times 10^4$ cells were placed to the upper chamber in 200 μL serum-free DMEM medium. The lower chamber contains 700 μL of medium containing 20% FBS. After incubated at 37°C for 30 h in migration assay or 50 h in invasion assay, the chambers were fixed by 4% paraformaldehyde for 30 min and stained with 0.1% crystal violet solution for 30 min. After being washed away the crystal violet, upper chamber cells were erased and then photographed by microscopy. Relative migration and invasion were quantified by ImageJ (v1.8.0).

### Bioinformatic analysis

The MS/MS data were processed using Maxquant search engine (v.1.5.2.8). Tandem mass spectra were searched with reverse decoy database. The mass tolerance for precursor ions was set as 20 ppm in First search and 5 ppm in Main search, and the mass tolerance for fragment ions was set as 0.02 Da. Wolfpsort (v.0.2) software was used to predict subcellular localization. MoMo (V5.0.2) software was used to analysis the model of sequences constituted with amino acids in specific positions of modify-21-mers (10 amino acids upstream and downstream of the site) in all protein sequences. For each category proteins, InterPro database was used to test the enrichment of the identified modified protein against all proteins of the species database by two-tailed Fisher's exact test. The ClusterProfiler (v4.2.2) package was used for function enrichment analysis. KEGG and GO biological process (BP), cellular component (CC), and molecular function (MF) terms were loaded from this package.

## QUANTIFICATION AND STATISTICAL ANALYSIS

GraphPad Prism (v8.0.2) software was used to performed statistical analysis. All the results are expressed as the mean values +/− SEM, * represents $p < 0.05$, ** represents $p < 0.01$, and *** represents $p < 0.001$. Statistical significance was defined as $p < 0.05$. Unpaired two-tailed Student's t test or one-way ANOVA test was used to performed quantitative analysis. All experiments were repeated at least three times.